Response to Anonymous Referee #1

Suski et al present single-particle mass spectrometry (SPMS) measurements of bacteria and fragments that served as CCN and INPs in the AIDA cloud chamber during immersion cloud freezing experiments. This work tackles the important question of the role of primary biological particles in cloud formation and properties through laboratory experiments. I have questions below regarding interpretation of the data that may impact the results. Otherwise, revisions are recommended below primarily to increase clarity of the manuscript. The main finding of this work is that bacteria fragments (mixed with agar) serve as cloud droplet nuclei, whereas intact bacteria rarely nucleate cloud droplets. The miniSPLAT size distributions of particles prior to cloud formation (expansion) within the chamber compared to the cloud droplet residuals support this conclusion. However, I have several questions that may impact the interpretation of the results.

Thank you for your detailed comments, suggestions, and questions. Below are our responses.

1) Could intact bacteria burst upon droplet activation or freezing? (Is there any support for this from previous studies?)

There is no evidence that bursting is occurring in the cloud chamber. If the intact cells were bursting during the expansion, they would not be observed post-expansion in roughly equal fractions as they were pre-expansion, as shown in the new Figure 7.

Or, could intact bacteria burst during drying within the CVI?

The aerosolized bacteria were dried prior to injection into the AIDA chamber; therefore, if bursting of these specific intact bacterial cells were to occur during drying, it should happen during this initial drying process as well. Consequently, it is unlikely that bursting occurs upon drying in the PCVI or IS-PCVI.

Moreover, if intact bacteria activate and then burst in the PCVI, we would expect to see an increase in the number of particles measured by the CPC that is downstream of the PCVI, similar to what is seen during aircraft flights when shattering of large droplets and ice crystals in CVIs occurs. These types of concentration spikes were not observed in the present study.

2) What are the size cuts of the PCVI and IS-PCVI and transmission efficiencies? This information needs to be provided in the experimental section. For each expansion, what fraction of the droplets and ice crystals were and were not transmitted through the CVIs? (Provide in results & discussion.)

The cut-sizes for the PCVI and IS-PCVI used in the 3 expansions have now been included on the expansion plots (Figures 4 9, and 13), as well as in Table S1 in the supplement. We have also calculated the fraction of droplets and ice crystals that were transmitted using the equation below and have plotted the fractions in Figure S1.

$$Fraction\ of\ the\ droplets\ and\ ice\ crystals\ reached\ at\ the\ CVI(t) = \frac{PCVI\ CPC(t) \times \frac{F_{output}}{F_{input}}}{Welas2(t)}$$

where F_{output} is the CVI output flow (lpm), and F_{input} is the CVI input flow (lpm).

Table S1 also lists the transmission efficiencies of 94.4% for Expansion 1 and 61.9% for Expansion 2 determined according to Figure 3 of Gallavardin et al. (2008) and 91.5% for Expansion 3 determined according to Fig. 13 of Hiranuma et al. (2016).

Gallavardin, S. J., Froyd, K. D., Lohmann, U., Möhler, O., Murphy, D. M., and Cziczo, D. J.: Single particle laser mass spectrometry applied to differential ice nucleation experiments at the AIDA chamber, Aerosol Sci. Tech., 42, 773–791, doi:10.1080/02786820802339538, 2008.

Hiranuma, N., Möhler, O., Kulkarni, G., Schnaiter, M., Vogt, S., Vochezer, P., Jarvinen, E., Wagner, R., Bell, D. M., Wilson, J., Zelenyuk, A., and Cziczo, D. J.: Development and characterization of an ice-selecting pumped counterflow virtual impactor (IS-PCVI) to study ice crystal residuals, Atmos Meas Tech, 9, 3817-3836, 10.5194/amt-9-3817-2016, 2016.

3) It is stated that the pressure changes during expansions impacted the miniSPLAT aerosol velocities. What was the dependence of the size dependent miniSPLAT inlet transmission efficiency on these pressure changes during expansions? If particles >0.5 um were not as efficiently transmitted through the aerodynamic lens at these lower pressures, this would explain why intact bacteria were not observed in the cloud particle residues.

The size-dependent transmission efficiency of the aerodynamic lens inlet, used by the AMS and miniSPLAT, is indeed expected to change with pressure. Liu et al. 2007 presents the results of CFD modeling and experimental data for sampling pressures of 760 torr and 585 torr. It shows that while the model predicts a decreased transmission efficiency for larger particles, measurements on 3 different particle types show virtually no change for the transmission efficiency of larger particles. The reference to this paper has also been added to the revised manuscript.

Most importantly, our measurements conducted during other expansions in the AIDA chamber show that when larger particles activate more efficiently, it can be clearly observed in the miniSPLAT-measured d_{va} distributions. For example, Figure 1 in the responses shows the normalized miniSPLAT-measured d_{va} size distributions measured before and during an expansion with feldspar present in the chamber. The size distribution of cloud residuals sampled during the expansion clearly shows an enhancement in the relative fraction of larger particles. This suggests that larger particles are effectively transmitted through the PCVI and the miniSPLAT inlet during expansions when pressures are lower than normal atmospheric pressure, consistent with the data reported in Liu et al. 2007.

Peter S. K. Liu , Rensheng Deng , Kenneth A. Smith , Leah R. Williams , John T. Jayne , Manjula R. Canagaratna , Kori Moore , Timothy B. Onasch , Douglas R. Worsnop & Terry Deshler (2007) Transmission Efficiency of an Aerodynamic Focusing Lens System: Comparison of Model Calculations and Laboratory Measurements for the Aerodyne Aerosol Mass Spectrometer, Aerosol Science and Technology, 41:8, 721-733, DOI: 10.1080/02786820701422278

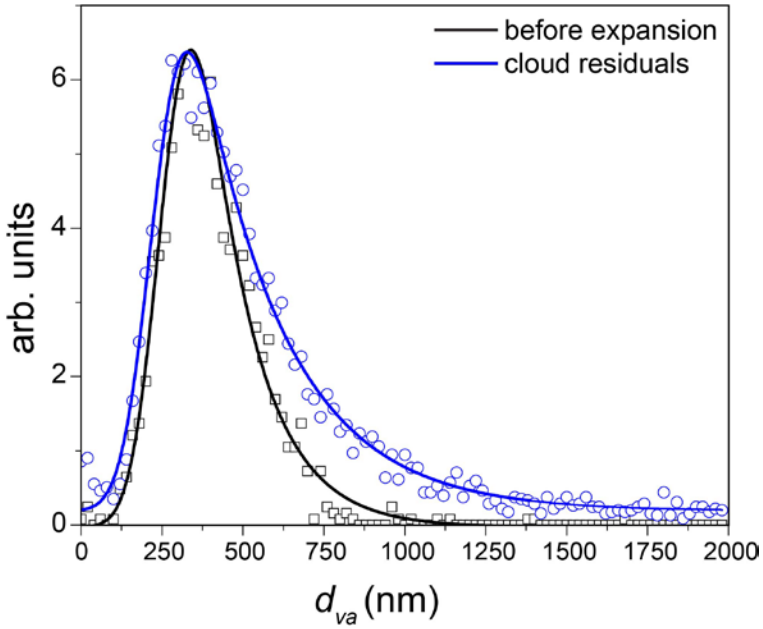

Figure 1.

Additional Major Comments:

- Experimental (Page 5): Please provide additional information about the miniSPLAT operation. What was the LDI power, and did it vary during the study (since ion fragmentation is dependent on this)?

The text has been modified to include this information. “The dual particle detection is also used to generate a trigger for the excimer laser (GAM Lasers Inc., Model EX-5), operated at 193 nm with a constant laser energy of 1.0 ± 0.1 mJ/pulse, which ablates the particles and generates positive and negative ions.”

What was the size dependent inlet transmission efficiency as a function of inlet pressure?

A full size-dependent transmission efficiency curve was not generated for each inlet pressure, but as discussed above, larger particles >0.5 um were transmitted during expansions. Figure 1 shows that the ratio of the two particle types measured by miniSPLAT before the expansion is consistent with the size distributions generated from the SMPS and APS. The important

issue here is the difference in the ratio of the concentrations of the two particle types before the expansion and of cloud residuals during the expansion. Size-dependent transmission efficiency curves for two pressures and 3 particle types are given in Liu et al. 2007 (Figures 9 – 11, Table 3). Using the data presented by Liu et al. in Table 3 we plotted their measured averaged transmission efficiencies for two pressures shown in Figure 2 in the response.

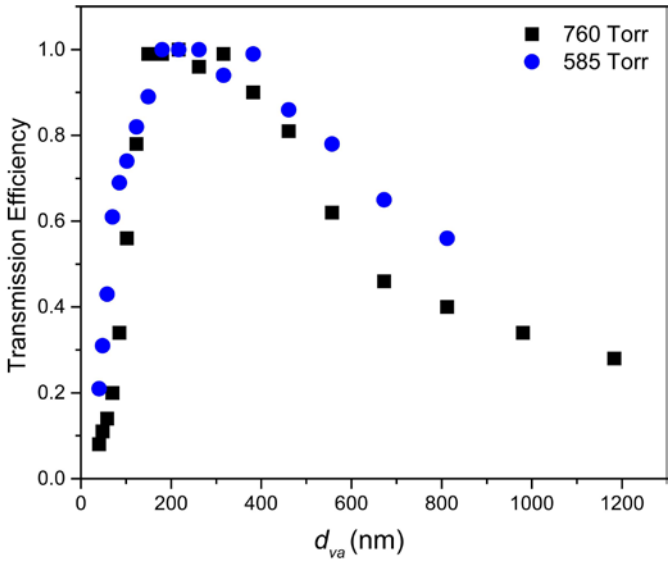

Figure 2.

The miniSPLAT size distributions measured before and after the expansions for the 3 experiments show two clear peaks for two particle types, while the cloud residual size distributions show that the large particle mode is missing. It is not that no large particles were detected in cloud residuals, they are clearly detected for other samples as explained above, but the distinct peak of the intact bacteria mode is not present.

Peter S. K. Liu , Rensheng Deng , Kenneth A. Smith , Leah R. Williams , John T. Jayne , Manjula R. Canagaratna , Kori Moore , Timothy B. Onasch , Douglas R. Worsnop & Terry Deshler (2007) Transmission Efficiency of an Aerodynamic Focusing Lens System: Comparison of Model Calculations and Laboratory Measurements for the Aerodyne Aerosol Mass Spectrometer, Aerosol Science and Technology, 41:8, 721-733, DOI: 10.1080/02786820701422278

How were size calibrations conducted (PSLs?) and over what particle size range?

This has been added to the text. “Given that the inlet pressure is changing during the expansions, polystyrene latex spheres (PSLs) of known sizes ranging from 73 nm to 993 µm were used to generate a pressure dependent size calibration curve over a range of pressures from 0.9 to 4 Torr.”

What is the size range of efficient inlet transmission, and does it depend on pressure? (Figure 1 only gives a lower detection limit – no upper limit is provided, although it is clear in this figure that transmission appears to drop off above 1 um.)

The size-dependent transmission efficiency of the inlet used in the SPLAT II and miniSPLAT instruments at normal atmospheric pressure is provided in Zelenyuk et al. (2009). Liu at al. (2007) reports measured size-dependent transmission efficiencies at 2 sampling pressures (Response Figure 2). Our measurements conducted during other expansions in the AIDA chamber show that ~micron-sized particles like feldspar that activated as CCN and/or IN are transmitted and detected by miniSPLAT.

Zelenyuk, A., Yang, J., Choi, E., Imre, D. (2009). SPLAT II: An Aircraft Compatible, Ultra-Sensitive, High Precision Instrument for In-Situ Characterization of the Size and Composition of Fine and Ultrafine Particles. Aerosol Science and Technology 43:411-424.

Peter S. K. Liu , Rensheng Deng , Kenneth A. Smith , Leah R. Williams , John T. Jayne , Manjula R. Canagaratna , Kori Moore , Timothy B. Onasch , Douglas R. Worsnop & Terry Deshler (2007) Transmission Efficiency of an Aerodynamic Focusing Lens System: Comparison of Model Calculations and Laboratory Measurements for the Aerodyne Aerosol Mass Spectrometer, Aerosol Science and Technology, 41:8, 721-733, DOI: 10.1080/02786820701422278

How were number concentrations obtained from the miniSPLAT data (what calibration/data processing was done)?

This has been added to the text for clarity. “miniSPLAT-measured particle number concentrations are calculated by dividing the particle detection rate at the first optical detection stage by the pressure-dependent sampling flow rate as described in detail in Vaden et al. (2011a).” This approach was previously applied to aircraft-based measurements and resulted in an average difference of 0.5% between 1-sec concentrations measured by miniSPLAT and a dedicated particle counter (Vaden et al. (2011a)).

- Page 5, Line 31: In addition to different relative peak intensities, there appear to be differences in the individual ions present at > m/z 50. This should be discussed.

It is easier to compare the mass spectra of the two particle modes using the new Figure 3 (original Figure S1), in which the lower intensity peaks are magnified. It shows that the mass spectra of the two particle types in the chamber have the same mass spectral peaks, just with different relative intensities.

- To aid interpretation of the mass spectra, please label all ions in Figures 2, 5, 7, 10, and 14. If the chemical identity is not known, please list possibilities and/or at least the numerical m/z.

In the new version of the paper these figures include labeled mass spectral peaks.

Also, please label in the captions whether these mass spectra correspond to averages or representative examples.

They are averages. A note was added to the figure captions.

- Figure S1 is a very informative figure, and the authors may consider moving this to the main text. In particular, the labeling of the ions is useful, and the magnification of the small peaks is helpful. Regarding the comparison here, what differences are observed between the 'agar + bacterial fragments' and 'agar'? This should be discussed in the main text to support the inclusion of agar in the aerosols (Page 6, Line 8). It appears that the main difference may be the presence of m/z 131 in the bacterial fragments. Is this observed in the aerosols and cloud residues? The mass spectra shown in the main text are only shown up to m/z 120, so the reader cannot evaluate this. If m/z 131 is indeed a primary difference between the mass spectra, then I recommend that the authors show the mass spectra in the main text up to at least m/z 135.

We have moved this figure to the main text. Both aerosolized intact bacteria and bacteria fragments mixed with agar are composed of the same compounds, albeit present in different ratios. Therefore, it is not surprising that the mass spectra of all particles in the chamber have the same mass spectral peaks just with different relative intensities, as shown in the new Figure 3. All of these particles, however, contain distinct phosphorus-containing peaks that separate them from pure agar. The peak at m/z 131 (possibly, $C_7H_{17}NO$) also appears to be characteristic of bacteria and of bacterial fragments.

Additionally, one of the findings presented in this manuscript is that the fraction of agar and bacterial fragments is changing with particle size. Figure 12 of the revised manuscript and Figure 3 in the response clearly illustrate this point. The simultaneous measurements of single particle composition *and* size provides the means to distinguish between the two particle types. However, distinguishing between intact bacteria and large particles composed of bacterial fragments mixed with agar based on their mass spectra is impossible.

- Page 6, Line 3: It is stated here that "intact cells show relatively lower intensities for the metal ions (23Na+, 39/41K+, 40Ca+)", but I do not see this in Figure 2.

The mass spectra shown in Figure 2 are normalized to the most intense peak (K^+). The intensity of this peak for intact bacteria represents a much lower fraction of the total mass spectral intensity (sum of all red peaks) as compared to the bacteria fragments mixed with agar.

Figure 3 in the response shows the size-dependent mass spectra of bacterial fragments mixed with agar, which were normalized by the total MS intensity. It clearly shows that the relative intensity of K^+ decreases with particle size.

Similarly, Figure 12, which used to be Figure 11 in the original version, provides another display of the decreasing relative intensity of the K peak with particle size.

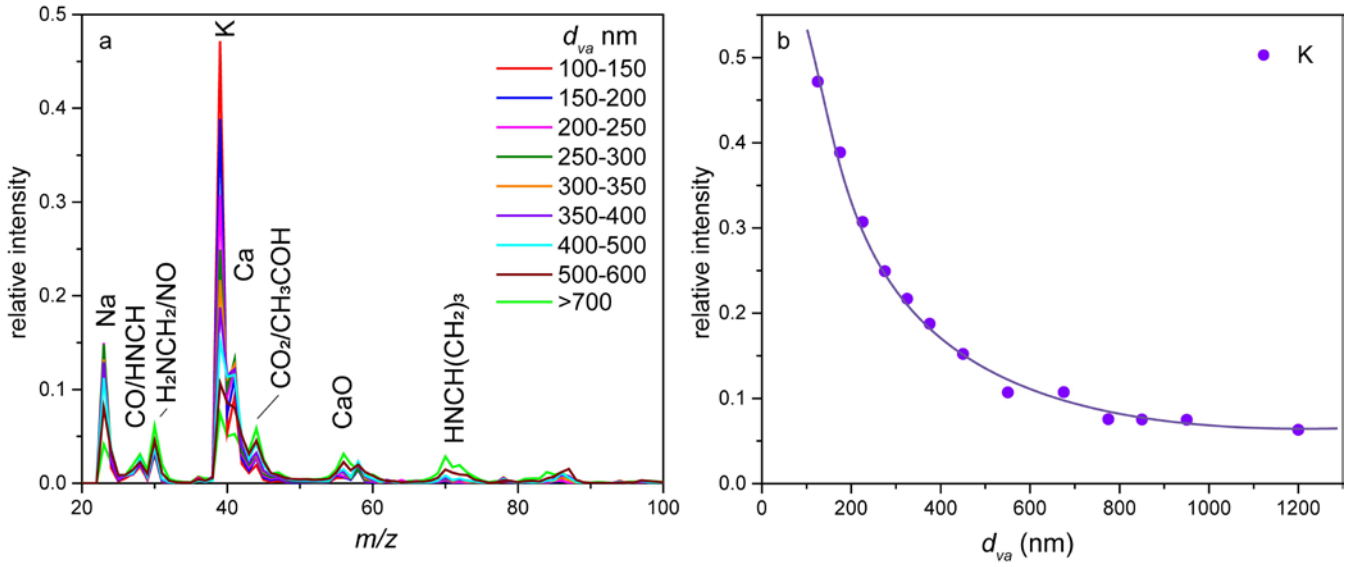

Figure 3.

- Page 6, Line 4: Please discuss the organic ions present, as they are not stated here in terms of m/z or ion formula, making interpretation of this statement by the reader not possible. There are many previous SPMS papers on primary biological particles that could aid in this mass spectral interpretation. A greater interpretation of the ions above m/z 41 may aid in the interpretation of the results. Example manuscripts to consult for SPMS biological particle mass spectra include (but are not limited to): Fergenson et al 2004 (Analytical Chem), Czerwienec et al 2005 (Analytical Chem), Srivastava et al 2005 (Analytical Chem). Peaks unique to the bacteria (fragments and intact) and not agar should be highlighted in this discussion.

We have expanded this discussion to include more ion identification.

- Page 7, Lines 23-25: It is stated here that "The small differences between the MS of residuals and the small particle mode suggest a slightly higher content of organics in the residuals", but I do not see this in Figure 5. Please provide additional support/description (e.g. label and discuss specific peaks).

We have added more information about the organic ions in the mass spectra and expanded the discussion.

- Page 9, Line 3: This sentence implies that peaks > m/z 44 are all organics, which contradicts Page 6, Lines 1-2 and previous SPMS biological particle studies that show higher mass inorganic peaks as well. This discussion should consider specific peaks and fix this statement.

We have revised this discussion and modified the original Figure 11 (new Figure 12). There are a number of ways to illustrate that the K^+ peak intensity relative to organic peaks decreases with particle size. Figure 12 and Figure 3 in the response, all illustrate this important point.

One of the important findings presented in this paper is that the relative concentrations of agar and bacterial fragments in the small particle mode change with particle size, such that the fraction of agar decreases with particle size.

- Page 9, Lines 28-30: Typically CVIs concentrate cloud residuals during sampling and this transmission is size-dependent. This information needs to be stated in the experimental section, and this needs to be considered in the interpretation of the number concentrations measured after the CVI, as discussed on this page. The reader also does not have knowledge of the transmission differences between the IS-PCVI and PCVI to evaluate the transmission of cloud droplets vs ice crystals as stated here.

The transmission efficiencies and cut-sizes have been added to the text. The size dependent concertation factor would be based on droplet or ice crystal size and not residual size. Therefore, calculating the size dependent residual enhancement is not relevant. Average particle concentration enhancement factor is calculated according to Eqn. 6 of Hiranuma et al. (2016) and was 2 for the PCVI and 12 for the IS-PCVI. This information has also been added to the text and the table in the supplement.

- Page 11, Line 31 – Page 12, Lines 1-2: This result was not shown or discussed in the results & discussion, and if included here in the conclusions, it should be shown and discussed.

This result is from unpublished data, so we have added a reference to a personal communication for this result. The n_s value for agar is 7.82 x 10^8 m^{-2} at -22.95 °C (250.20 K).

- To aid in comparison of the results between the different expansions, the authors are encouraged to combine (into a multi-panel plot or by stacking the mass spectra) the following mass spectral figures: 5, 7, 10, and 14. Similarly, interpretation would be improved with combining the following size distribution figures: 4, 9, and 13. Figures 1 and 6 could be similarly combined.

We find that data in combined multi-panel plots are difficult to comprehend and interpret.

Most importantly, we chose to present the results as three *separate* experiments to emphasize that the data from three separate experiments and two different bacteria are perfectly reproducible.

- Figure 11 and associated discussion: Since ion intensities in laser desorption ionization are dependent on ionization energies (e.g. Gross et al 2000, Analytical Chem.; Reinard & Johnston 2008, J. ASMS), the ion ratios used here need to be discussed in greater detail as they do not represent quantitative mole or mass ratios. In particular, inorganic ions typically have much lower ionization efficiencies compared to organic ions, which also undergo significant fragmentation at 193 nm. In addition, the organic ions included here in the ratio need to be stated here, in the experimental, or in the results & discussion. While it is clear that the organic contribution increases with size (and this is a useful result), clarification needs to be provided for the reader not familiar with LDI. Additionally, the text on page 9 refers to the dva distribution here as a 'schematic representation'. Please clarify in the caption and show actual data instead.

The revised figure (new Figure 12) shows the actual dva distribution. As we discussed above, there are a number of ways to illustrate that the intensity of the K^+ peak relative to organic peaks decreases with particle size. Figure 12 and Figure 3 in the response, all illustrate this important point. The text also clearly states that the ratios presented in Figure 12 serve as a simple ***qualitative*** measure of the relative fraction of bacterial fragments and agar in these particles. We have modified the text to clarify how the ratio shown in the figure was calculated.

We agree that this is one of the important findings in this study.

Minor Comments:

- Introduction: Many sentences do not include references, which should be added to support the statements. In particular, references are needed on page 2, lines 1, 12, 14, 20, and 21.

References have been added to these sentences.

- Page 3, Line 23: Move this sentence to the end of the previous paragraph, as one sentence does not constitute a full paragraph.

It has been moved.

- Page 4: RH is defined twice here as well as on page 2.

This has been fixed. Thank you.

- Page 4, line 15: Why are the SMPS and APS data converted to volume-equivalent diameters? It would seem more appropriate, for comparison to the miniSPLAT data (in vacuum aerodynamic diameter), to simply convert the SMPS mobility diameters to aerodynamic diameter and leave the APS data in aerodynamic diameter. Also, please provide a reference for the chosen particle density.

A similar application of volume equivalent diameter in SMPS and APS data for other studies in the AIDA chamber can be found in Hiranuma et al 2015 (Nature Geosci.; DOI: 10.1038/NGEO2374, See Supplemental Information Section 1.3) and many other publications. In addition, the volume-equivalent diameter was used for the SMPS/APS data to be comparable to Welas2-measured metrics (e.g., Hiranuma et al., 2015; Atmos. Chem. Phys., 15, 2489–2518, 2015). Sect. 3.4 of Hiranuma et al. (2016) and references therein describe why volume-equivalent diameter is the best choice for displaying welas2 data, but briefly it is because we do not know the geometry of the ice crystals. The density of 1.4 g/cm^3 was used here to arrive at a good overlap in the SMPS and APS size distributions, assuming particle sphericity (Peters et al. (2006)). We have added more clarification on this in the text.

The effective density of this bacteria of 1.4 g cm^{-3} has been previously measured in Wex et al. 2015 and is in a good agreement with the effective density of 1.38 g cm^{-3} measured by miniSPLAT for intact pseudomonas syringae during the FIN-1 campaign.

Moreover, the vacuum aerodynamic diameter measured by miniSPLAT is not the same as aerodynamic diameter measured by APS. What is important for this study is that 2 distinct particle modes are clearly visible in the miniSPLAT and SMPS/APS-measured size distributions.

Hiranuma, N., Möhler, O., Kulkarni, G., Schnaiter, M., Vogt, S., Vochezer, P., Jarvinen, E., Wagner, R., Bell, D. M., Wilson, J., Zelenyuk, A., and Cziczo, D. J.: Development and characterization of an ice-selecting pumped counterflow virtual impactor (IS-PCVI) to study ice crystal residuals, Atmos Meas Tech, 9, 3817-3836, 10.5194/amt-9-3817-2016, 2016.

Wex, H., Augustin-Bauditz, S., Boose, Y., Budke, C., Curtius, J., Diehl, K., Dreyer, A., Frank, F., Hartmann, S., Hiranuma, N., Jantsch, E., Kanji, Z. A., Kiselev, A., Koop, T., Möhler, O., Niedermeier, D., Nillius, B., Rosch, M., Rose, D., Schmidt, C., Steinke, I., and Stratmann, F.: Intercomparing different devices for the investigation of ice nucleating particles using Snomax (R) as test substance, Atmos Chem Phys, 15, 1463-1485, 10.5194/acp-15-1463-2015, 2015.

Peters, T. M., Ott, D. & O'Shaughnessy, P. T. Comparison of the Grimm 1.108 and 1.109 388 portable aerosol spectrometer to the TSI 3321 aerodynamic particle sizer for dry particles. 389 *Annals of Occupational Hygiene*, **50**, 843–850, doi:10.1093/annhyg/mel067 (2006).

- Results & Discussion: It would be useful for the reader for sub-headers to be added, for example, 1) Bacteria mass spectral signatures, 2) Expansion 1, 3) Expansion 2. . ..

We have added sub-headers to the text.

- Page 5, Line 18: Space needed after (dve).

This has been fixed.

- Page 6, Lines 11-13: This sentence is not clear as written. Laser power should be provided in the experimental section.

This has been clarified as "The negative ion MS presented here and in previous studies are virtually the same, while the positive ion MS presented in this study exhibit significantly higher intensity in organic peaks, most likely due to the differences in the ablation laser power or wavelength (266 nm in Pratt et al. (2009) and 193 nm in this study and Zawadowicz et al. (2017)). Moreover, these studies do not mention the presence of two particle size modes nor distinguish between their mass spectra." Also, laser power is now listed in the experimental section.

- Page 7, Lines 26-27: Move this sentence to later in the results & discussion where Expansion 2 is discussed.

We feel that this sentence is important. We have it here to inform the reader that we will explain this result in more detail later on in the text.

- Page 7, Last paragraph: This paragraph is all repetition (summary) and could be removed as it doesn't seem necessary.

Thank you for the suggestion. We did remove many repetitive sentences in the revised manuscript.

- Page 9, Lines 7-10: Please clarify this sentence.

This has been rewritten to read, "To examine this further, we compare in Figure S2a the MS of cloud residuals smaller than 300 nm to the reference MS of the small particle mode measured before the expansion and find them to be nearly identical. This indicates that they are bacterial fragments mixed with agar. The MS of cloud residuals that are larger than 300 nm have greater ion intensities for the organic peaks ($^{28}CO/HNCH^+$, $^{44}CO_2/CH_3COH^+$, $^{70}HNCH(CH_2)_3^+$, $^{85}C_5NH_{10}^+$) than the bacterial fragments mixed with agar, but slightly smaller ion intensities than those of the reference MS of intact bacteria, as shown in Figure S2b. These differences in ion intensities are not sufficient to eliminate the possibility that some of the larger cloud residuals could be smaller intact bacteria."

- Page 9, Line 19: Should Figure 13 be referred to here instead of Figure 6a (typo?)?

No, the correct figure is referenced.

- Page 9, Line 24: Add mention of the number concentration prior to expansion for context.

The text has been revised to read, "Figure 13c displays the welas2-measured total number of activated particles as a function of time (black), which reaches a maximum of ~700 particles cm^{-3}. Before the expansion, 1456 cm^{-3} particles were present in the chamber indicating that 47% of the particles activated as CCN."

- Page 10, Lines 3-4: Move "(light blue)" to after "expansion" in this sentence.

It has been moved.

- Page 10, Lines 10-12: Move sentence to the end of the previous paragraph.

These sentences have been combined with the next paragraph, not with the previous, because the previous paragraph is about size distributions and these sentences are about the mass spectra.

- Page 11, Line 23: Please provide a reference for the hygroscopicity of intact bacteria.

A reference has been added.

- Figure 9 caption: Mention the type of bacteria used. Make sure this is included in each figure caption.

This information has been added to all figure captions.

- Figure 12: Please clarify the legend of the bottom plot.

The blue trace has been added to the legend.

- Figure 13: Please provide the sample timing for the 'cloud residuals' vs 'cloud residuals late', so that the reader can refer back to Figure 12 for context.

This has been added to the text and the figure caption.

Response to Anonymous Referee #2

Thank you for your comments and suggestions. We have addressed them in the revised version of the paper. Below are our responses to your comments.

-Suski et al. present experimental data from three cloud chamber expansions at AIDA where a suspension of bacterial particles and their fragments mixed with agar were injected into the chamber. The goal appears to be to understand and contrast the role of intact bacterial cells versus bacterial fragments mixed with agar in the nucleation of cloud droplets than can then undergo immersion freezing. This is certainly a relevant question to the atmospheric science community, though the presence of agar makes the results more relevant to interpreting past and future laboratory studies that use nebulized suspensions of bacterial since agar is not an atmospherically relevant particle component.

In the end few new findings are really presented from these experiments, and the significance and originality of this work is rather low as a result. Perhaps the most novel aspect is the use of a cloud expansion chamber.

The main finding is that intact bacterial particles make a small contribution to CCN activation and thus cloud droplets, and thus also a small contribution to immersion freezing and ice crystal production. This is certainly a worthwhile finding and it should really be made the focus of this paper, but it also requires better support from the available data.

The reviewer clearly came to the conclusion that the paper presents data which indicates that particles composed of bacterial fragments mixed with agar activated to form either droplets or ice crystals much more efficiently than intact bacteria. As the referee notes, this *is* an important finding. Agar or other growth media is present in ***all*** laboratory studies that are done with cultured bacteria and the present study shows that it plays an important role that needs to be considered when interpreting CCN and IN activation data. To the best of our knowledge, we present the 1st measurements of both size distributions and composition of cloud residuals of these bacteria, which made it possible to identify which particles were preferentially activated. As we note in the paper, not knowing which particles were activated led some previous studies to calculate the fractions of particles that activate as droplets and ice crystals relative to the number of intact bacteria only or to the total number of particles in the chamber. Each of these choices led to INP/CN values that do not accurately describe the activity of either particle type.

Another important new finding in this study is that the relative fraction of agar in these particles gradually decreases with particle size, which affects their hygroscopicity and hence CCN and IN activity.

-I also found the paper hard to follow, and do not think the very narrative style of discussing each of the three cloud expansions to be an effective way to communicate, analyze, and synthesize the results.

We have revised the paper to improve the flow, better illustrate the key points, and address reviewer's concerns. We also have added Table S1 that lists experimental parameters for the 3 expansions, including the CCN/CN and INP/CN ratios.

-I was not very convinced by the interpretation of these results, especially since the intact bacterial were such a small contribution to the total particle numbers to begin with. The single-particle mass spectrometer SPLAT is used to determine the chemical composition as a function of size. This analysis is hampered by the lack of significantly distinct mass spectral features that can be used to reliably distinguish the fragment+agar particles from the intact bacteria. As it is a single-particle instrument, as droplet and ice crystal activation occurs on individual particles, I found it odd that average mass spectra were presented, as opposed to trying to determine the fraction of each type of particle as a function of particle size.

It is important to keep in mind that in most previous laboratory studies of aerosolized cultivated bacteria the fraction of intact bacteria was small. Our paper is the first study that shows which of the particle types were activated as CCN and INP more efficiently when both intact bacteria and fragments mixed with agar are present at the same time.

Aerosolized intact bacteria and bacterial fragments mixed with agar are composed of the same compounds, albeit present in different ratios. Therefore, it is not surprising that individual mass spectra of all particles in the chamber have the same mass spectral peaks, as shown in the new Figure 3, just with different relative intensities. All of the bacteria and bacterial fragment particles, however, contain distinct phosphorus-containing peaks that separate them from pure agar.

Additionally, we demonstrate for the first time that the relative fractions of agar and bacterial fragments are changing with particle size, thereby, effecting their mass spectra. Figure 12 of the revised manuscript and Figure 3 in the response to reviewers clearly illustrate this point. As a result, distinguishing between intact bacteria and large bacteria fragments mixed with agar based on their mass spectra alone is impossible. However, a clear distinction between these two particle types is clearly seen in the particle size distributions that show two distinct peaks, one at ~180 nm and the other at ~850 nm (d_{va}). Simultaneous measurements of single particle composition *and* size provides the means to compare CCN and IN efficiency of two particle types.

The fact that there were more particles composed of bacterial fragments mixed agar than intact bacteria does not invalidate the results. An examination of the size distributions shows that the vast majority of particles larger than 600 nm (d_{va}) are intact bacteria. Inspection of the d_{va} size distributions of activated particles, which does not show the distinct peak that corresponds to intact bacteria, clearly indicates that under the experimental conditions in the AIDA chamber, in which not all particles activate as cloud droplets (Table S1), the more hygroscopic smaller particle mode, composed of bacterial fragments mixed with agar, activate with significantly higher probability than intact bacteria.

-In summary, while the topic is of interest, not much new insight is presented here, and the presentation and discussion is quite unclear and hard to follow. The main singular conclusion that intact bacteria do not activate as CCN or into ice crystals needs further support. Extensive revisions are required to achieve this, and publication in ACP may not be warranted unless these major issues can be properly resolved.

We chose to present three *separate* experiments conducted on two bacteria to demonstrate that the data, and hence the conclusions, are perfectly reproducible. Nevertheless, we have revised the paper to improve the flow and better illustrate the key findings.

We agree that given the importance of this topic the findings, which were reported here for the first time, call for follow-up studies.

-I find the narrative style of describing each expansion experimental chronologically to be an ineffective way to communicate the results. At the least the important characteristics of each expansion and how they differ from each

other must be discussed. E.g. how do the aerosol concentrations and size distributions differ? How do the thermodynamic conditions of the expansion differ? It looks like expansion 1 reaches a higher supersaturation of at least 102% RHw. Stating the maximum SS/RHw reached in each expansion is critical for understanding the CCN activation, just as stating the maximum RHi and minimum temperature reached is critical for understanding the ice crystal production.

In addition to presenting all of the RH data in the figures, we have added a table to the supplemental section (Table S1) that includes all of the expansion details.

We chose this narrative style to emphasize the fact that the results of these three separate experiments, on two different bacteria, are perfectly reproducible. The differences between the thermodynamic conditions of the three expansions were minor. We agree with the reviewer that the issue of the precise value of SSw/RHw is central to most CCN and IN activation studies from which parameters for models are being calculated. This, however, is not the goal of the present study. Below, we will return to the discussion of RHw measurements.

-We note that the reviewer concludes the review by stating (copied from below): **"Nevertheless, the data presented here show that bacterial fragments mixed with agar preferentially activate as droplets and are the only particles observed in ice residuals." This is essentially the singular conclusion reached from this study, and it is an interesting one. I strongly suggest making this aspect the focus and providing more data and analysis that better supports this conclusion.**

We agree with this conclusion. We have also revised the manuscript and added the additional data you requested.

-In describing each expansion, the authors mostly state what data is plotted in the various figures, as opposed to actually discussing, interpreting, and synthesizing the results. As written the description of the expansion experiments is not very meaningful.

We have revised the discussion to more clearly convey our interpretations of the results.

-On "hydrophobic" intact bacterial particles. So long as the particle surface is wettable these large particles will still activate under the high supersaturations reached here. It appears that RHw usually hits 101%, so 1% SS. This is why it is important to state the maximum RHw. At high a high SS large particles with a very small hygroscopicity of kappa ~ 0 will still activate into droplets.

The revised plots show the raw 1-sec data from tunable diode laser (TDL), which was used for in-situ measurements of the water vapor concentrations using absorption spectroscopy throughout the expansions. As discussed in detail elsewhere, (e.g. Fahey et al. (2014; www.atmos-meas-tech.net/7/3177/2014/); Hiranuma et al., 2014a (www.atmos-chem-phys.net/14/13145/2014/)) the accuracy of the measured relative humidity with respect to water (RHw) and ice (RHi) is ± 5 %. In the three expansions presented here the maximum values of the measured RHw were 97% for expansion 1, and 96% for the other two (Table S1). Given that cloud droplets were clearly formed, the values of RHw in the original plots were scaled.

The high uncertainties in the RH measurements make it impossible to precisely determine SSw, which is necessary to calculate particle hygroscopicity parameters; however, this was not the goal of the present study. Again, the questions at hand are, which of the two particle types are more CCN and IN active under the same conditions, and does agar play an important role?

The CCN/CN ratios listed in Table S1 indicate that not all particles in the chamber activated as cloud droplets, providing a possible explanation for why the more hygroscopic bacterial fragments mixed with agar activate, while the less hygroscopic intact bacteria do not.

-What would really help this analysis is if the /fraction/ of the two type types/size modes of particles that activate into cloud droplets and ice crystals in each expansion could be estimated. This should be possible from the data.

We calculated the fractions of particles that activated into cloud droplets and ice crystals in all three expansions and provided this information in Table S1 and in the text. Since it is impossible to distinguish between intact bacteria and large bacteria fragments mixed with agar, we cannot calculate the fraction of intact bacteria that act as CCN and INP based on MS alone. However, the size distributions of cloud residuals, shown in Figures 5, 10 and 14, exhibit no distinct peak for intact bacteria and are dominated by smaller particles composed of bacterial fragments mixed with agar.

-It is rather misleading to say that the intact bacteria make a small contribution to cloud droplets and ice crystals considering they are a small fraction of the initial particles to begin with.

The fractions of the intact bacteria in these experiments are rather typical for laboratory studies on cultivated bacteria (e.g. Wex et al., 2015;Wolf et al., 2015;Möhler et al., 2008).

If intact bacteria were, as typically assumed, more active than the bacterial fragments mixed with agar, they would be relatively enhanced in cloud residuals. Such enhancement would yield a more prominent peak at ~850 nm in the d_{va} size distributions, as compared to the peak observed for the particles before the expansions.

We clarified the text to say that relative to the bacterial fragments mixed with agar the fraction of intact bacteria, if present in activated particles, is much smaller than that in the original sample.

Wex, H., Augustin-Bauditz, S., Boose, Y., Budke, C., Curtius, J., Diehl, K., Dreyer, A., Frank, F., Hartmann, S., Hiranuma, N., Jantsch, E., Kanji, Z. A., Kiselev, A., Koop, T., Möhler, O., Niedermeier, D., Nillius, B., Rosch, M., Rose, D., Schmidt, C., Steinke, I., and Stratmann, F.: Intercomparing different devices for the investigation of ice nucleating particles using Snomax (R) as test substance, Atmos Chem Phys, 15, 1463-1485, 10.5194/acp-15-1463-2015, 2015.

Wolf, R., Slowik, J. G., Schaupp, C., Amato, P., Saathoff, H., Möhler, O., Prevot, A. S. H., and Baltensperger, U.: Characterization of ice-nucleating bacteria using on-line electron impact ionization aerosol mass spectrometry, J Mass Spectrom, 50, 662-671, 10.1002/jms.3573, 2015.

Möhler, O., Georgakopoulos, D. G., Morris, C. E., Benz, S., Ebert, V., Hunsmann, S., Saathoff, H., Schnaiter, M., and Wagner, R.: Heterogeneous ice nucleation activity of bacteria: new laboratory experiments at simulated cloud conditions, Biogeosciences, 5, 1425-1435, 2008.

-What is needed are the particle fractions, ie the CCN/CN and INP/CN ratios. This will also make these results more useful in a quantitative manner for other researchers.

These have been added to the paper and listed in Table S1.

-As presented the results reported here cannot be used in a meaningful to for example describe the CCN or IN properties of these particles types in a model.

The goal of this manuscript is not to calculate the CCN and IN fractions to be used in a model. As we discuss in the paper, the size, number concentration, and relative fraction of the small particles containing bacterial fragments mixed with agar are affected by the solution/suspension concentrations of agar, intact bacteria, and cell fragments, how old it is, as well as how the bacteria culture was grown and prepared.

Future studies need to be aware of the unavoidable presence of agar or other growth media that can greatly change the results. We cannot overemphasize that in order to use laboratory studies to generate useful parameters for atmospheric models one

must make sure to eliminate artifacts that can affect CCN and IN activity. In the case of cultured bacteria, agar or other growth media is present in all laboratory studies and its effect makes it impossible to extrapolate the data to atmospheric conditions, where no agar is expected.

-Pg 1/line 30: Please provide several references for this b/g info on the role of bacteria in the atmosphere and clouds. "Murray, 2012 and references therein" is not sufficient.

One suggestion:

DeMott, P. J. and Prenni, A. J.: New Directions: Need for defining the numbers and sources of biological aerosols acting as ice nuclei, Atmos. Environ., 44(15), 1944–1945, doi:10.1016/j.atmosenv.2010.02.032, 2010.

References have been added.

-2/7: Contact angle would explain only the wettablilty, not hygroscopicity, of bacteria. Hygroscopicity really refers to the ability of a dissolved solute solution to take up water.

To the best of our knowledge there are no papers on the hygroscopicity of intact bacteria. The contact angle measurements were used to infer hygroscopicity in the referenced study.

-2/15: The introduction is quite spare on references to the many prior papers on the ice nucleation properties of bacteria/Pseudomonas syringae/Snomax. Some of these get mentioned much later in the paper but they also belong in the introduction, or else it appears that the authors are not familiar enough with the topic under study here. Some suggestions, but there are many more:

Pandey, R., Usui, K., Livingstone, R. A., Fischer, S. A., Pfaendtner, J., Backus, E. H. G., Nagata, Y., Frohlich-Nowoisky, J., Schmu ser, L., Mauri, S., Scheel, J. F., Knopf, D. A., Po schl, U., Bonn, M. and Weidner, T.: Ice-nucleating bacteria control the order and dynamics of interfacial water, Sci. Adv., 2(4), e1501630–e1501630, doi:10.1126/sciadv.1501630, 2016.

Lindow, S. E., Arny, D. C. and Upper, C. D.: Bacterial Ice Nucleation: A Factor in Frost Injury to Plants, PLANT Physiol., 70(4), 1084–1089, doi:10.1104/pp.70.4.1084, 1982.

Després, V., Huffman, J. A., Burrows, S. M., Hoose, C., Safatov, A., Buryak, G., Fröhlich-Nowoisky, J., Elbert, W., Andreae, M., Pöschl, U. and Jaenicke, R.: Primary biological aerosol particles in the atmosphere: a review, Tellus B Chem. Phys. Meteorol., 64(1), 15598, doi:10.3402/tellusb.v64i0.15598, 2012.

Polen, M., Lawlis, E. and Sullivan, R. C.: The unstable ice nucleation properties of Snomax® bacterial particles, J. Geophys. Res. Atmos., 121(19), 11,666-11,678, doi:10.1002/2016JD025251, 2016.

Wex, H., Augustin-Bauditz, S., Boose, Y., Budke, C., Curtius, J., Diehl, K., Dreyer, A., Frank, F., Hartmann, S., Hiranuma, N., Jantsch, E., Kanji, Z. A., Kiselev, A., Koop, T., Möhler, O., Niedermeier, D., Nillius, B., Rösch, M., Rose, D., Schmidt, C., Steinke, I. and Stratmann, F.: Intercomparing different devices for the investigation of ice nucleating particles using Snomax® as test substance, Atmos. Chem. Phys., 15(3), 1463–1485, doi:10.5194/acp-15-1463-2015, 2015.

Pummer, B. G., Bauer, H., Bernardi, J., Bleicher, S. and Grothe, H.: Suspendable macromolecules are responsible for ice nucleation activity of birch and conifer pollen, Atmos. Chem. Phys., 12(5), 2541–2550, doi:10.5194/acp-12-2541-2012, 2012.

Turner, M. A., Arellano, F. and Kozloff, L. M.: Components of ice nucleation structures of bacteria, J. Bacteriol., 173(20), 6515–6527, 1991.

Turner, M. A., Arellano, F. and Kozloff, L. M.: Three separate classes of bacterial ice nucleation structures, J. Bacteriol., 172(5), 2521–2526, 1990.

Attard, E., Yang, H., Delort, A.-M., Amato, P., Pöschl, U., Glaux, C., Koop, T. and Morris, C. E.: Effects of atmospheric conditions on ice nucleation activity of <i>Pseudomonas</i>, Atmos. Chem. Phys., 12(22), 10667–10677, doi:10.5194/acp-12-10667-2012, 2012.

Hartmann, S., Augustin, S., Clauss, T., Voigtländer, J., Niedermeier, D., Wex, H. and Stratmann, F.: Immersion freezing of ice nucleating active protein complexes, Atmos. Chem. Phys. Discuss., 12(8), 21321–21353, doi:10.5194/acpd-12-21321-2012, 2012.

Vali, G., Christensen, M., Fresh, R. W., Galyan, E. L., Maki, L. R. and Schnell, R. C.: Biogenic ice nuclei 2. Bacterial sources, J. Atmos. Sci., 33(8), 1565–1570, 1976.

Some of these papers were already in the introduction, but we have added the suggested references that were not there and expanded the introduction.

-2/23: Macromolecules of protein aggregates are known ice nucleants produced by bacteria. Are the macromolecules really a “solid nucleus”. This definition doesn’t align with the role of macromolecules as ice nucleants.

This has been revised to read, “In immersion freezing, the INP first activates as a liquid cloud droplet, when the RH over water (RH_w) exceeds 100% RH, and subsequently ice forms, which means that this ice formation mechanism is tightly connected to the particle CCN activity.”

-2/26: Consider using “macromolecules” instead of “nano-INP”, as this is the terminology more widely used.

It has been changed to macromolecules.

-3/3: There is also evidence of biological ice nucleating macromolecules attaching to particles such as dust, and also evidence for mixed “dust-bio” particles, such as from the first author’s prior work. This would also seem to motivate this study and should be discussed.

Sullivan, D., Murray, B. J., Ross, J. F. and Webb, M. E.: The adsorption of fungal ice-nucleating proteins on mineral dusts: a terrestrial reservoir of atmospheric ice-nucleating particles, Atmos. Chem. Phys., 16(12), 7879–7887, doi:10.5194/acp16-7879-2016, 2016.

This reference has been added and this point added to the introduction.

-3/27: It is a bit confusing that the stated purpose of FIN-1 is to intercompare SPMS instruments and yet that is not done here. Please explain more to better put this particular study in the context of FIN-1.

This discussion has been expanded. It now reads: “The Fifth International Ice Nucleation Workshop (FIN) was a three-part study that aimed to compare a number of single particle mass spectrometers and ice nucleation instruments. The data presented here were collected during FIN-1, which took place in November of 2014 at the AIDA cloud chamber at KIT in Karlsruhe, Germany. Ten single particle mass spectrometers from several research groups around the world were brought together for FIN-1 to simultaneously characterize the size and composition of various types of aerosol particles, including those being used in the AIDA chamber to study their activity as CCN and INPs, Various aerosol types were sampled from the AIDA cloud chamber before, during, and after expansions forming cloud particles and each of these mass spectrometers sampled using

their own protocol. The results of the intercomparison will be the subject of future publication. The present manuscript presents the results of measurements, made by miniSPLAT only, during three expansions using two bacteria. ”

It is important to point out that the extremely high detection efficiency and sensitivity of our SPMS, including its unmatched sensitivity to small particles, as well as its dual data acquisition mode, (Zelenyuk et al. 2015) makes it uniquely suitable to characterize both types of particles before, after, and during the expansions with high temporal resolution.

Zelenyuk, A., Imre, D., Wilson, J. et al. J. Am. Soc. Mass Spectrom. (2015) 26: 257. https://doi.org/10.1007/s13361-014-1043-4

-4/14: Usually the particle density and shape are varied to arrive at a good overlap in the SMPS and APS size distributions, instead of just assuming values. Also what are these assumed values based on? Isn't the SPLAT instrument a great way to actually measure the shape factor and density of these particles?

The values are not assumed. The effective density of the bacteria of 1.4 g cm^{-3} has been previously measured and presented in the paper referenced below. It was used here to achieve a good overlap of the SMPS and APS size distributions, assuming particle sphericity. We have added more clarification on this in the text. Moreover, this value is in a good agreement with effective density of 1.38 g cm^{-3} measured by miniSPLAT for intact pseudomonas syringae during the FIN-1 campaign.

Wex, H., Augustin-Bauditz, S., Boose, Y., Budke, C., Curtius, J., Diehl, K., Dreyer, A., Frank, F., Hartmann, S., Hiranuma, N., Jantsch, E., Kanji, Z. A., Kiselev, A., Koop, T., Möhler, O., Niedermeier, D., Nillius, B., Rosch, M., Rose, D., Schmidt, C., Steinke, I., and Stratmann, F.: Intercomparing different devices for the investigation of ice nucleating particles using Snomax (R) as test substance, Atmos Chem Phys, 15, 1463-1485, 10.5194/acp-15-1463-2015, 2015.

Khlystov, A., Stanier, C. and Pandis, S. N.: An Algorithm for Combining Electrical Mobility and Aerodynamic Size Distributions Data when Measuring Ambient Aerosol, Aerosol Sci. Technol., 38(sup1), 229–238, doi:10.1080/02786820390229543, 2004.

Beddows, D. C. S., Dall'osto, M. and Harrison, R. M.: An Enhanced Procedure for the Merging of Atmospheric Particle Size Distribution Data Measured Using Electrical Mobility and Time-of-Flight Analysers, Aerosol Sci. Technol., 44(11), 930–938, doi:10.1080/02786826.2010.502159, 2010.

-4/27: Please state the cut-size of these two CVIs.

This information has been added to the paper (Table S1 and Figures 4, 9, and 13).

-5/10: Why were these two cultures chosen? Much existing work of course on P. syringae, but what about PF CGina 01? Also unclear if these are both used in all three expansions?

Pseudomonas syringae and PF CGina are two different strains of *Pseudomonas* bacteria. PF CGina has been studied previously and has been shown to be an efficient INP at modestly supercooled temperatures. It has also been observed in glacier meltwater. More information about PF CGina has been added to the introduction to address this issue. Pseudomonas syringae was used in Expansion 1, while PF CGina was used in Expansions 2 and 3. The data presented in the paper indicate that the findings are consistent for both bacteria strains.

-6/15: Do you determine which particles are intact bacteria simply based on a size threshold, and if so what is it and what is it based on?

Yes, this is explained in the text. The particles in the AIDA chamber have 2 distinct size modes, with the larger size mode (d_{va} above ~700 nm) corresponding to intact bacteria.

-7/6: Qualitative terms such as "very high CCN activation efficiency" are often used. The hygroscopicity of the different aerosol types should be estimated from the maximum supersaturation observed, and the size distribution.

We have calculated the CCN/CN and have added it to the paper.

-7/14: Why would these large bacterial particle not activate? Again need to know the maximum in the RHw.

As the reviewer notes, the data presented here indicate that under these experimental conditions the large intact bacteria particles are ineffective CCN, which, in essence, implies that they are weakly hygroscopic. In contrast, smaller particles contain IN-active bacterial fragments and hygroscopic agar. Less than half of the particles in the AIDA chamber activated to form cloud droplets, thus there was competition for water vapor during the expansion or the SSw did not reach a high enough value to activate the less hygroscopic particles in the chamber. Here we are being asked to speculate as to why intact bacteria are less hygroscopic, which is beyond the scope of the present paper. We note that the interaction between water and live cells/bacteria and the mechanisms by which they prevent water from entering into the cell are the subject of many research papers.

The issue of the large uncertainties in the measured RHw in the AIDA chamber have been already discussed above.

-Have you tested that these large particles once activated into cloud droplets survive the PCVI? I agree with the other referee's comments regarding the bacterial possibly rupturing during cloud droplet activation and certainly during freezing.

The transmission efficiencies of droplets of this size have been characterized and are presented in Hiranuma et al., 2014a (www.atmos-chem-phys.net/14/13145/2014/). However, bacteria bursting in the PCVI has not been tested directly in this study, but it is not clear what the mechanism for not surviving the PCVI would be.

The data do not support the idea that intact bacteria burst upon drying in the PCVI: (a) The bacteria do not all burst upon drying, as they were all dried prior to injection into the chamber and we still see intact bacteria in the chamber; (b) If they burst in the PCVI, we would expect to see a large increase in the number of particles measured by the CPC downstream of the PCVI, which was not observed; (c) Intact bacteria do not all burst upon activation or freezing because after the expansion there are still intact bacteria present in the cloud chamber. In addition, the ratio of the two particle types remain constant in the size distributions before and after the expansion, as shown in Figure 7. Therefore, we conclude that the evidence suggests that the idea of bursting intact bacteria does explain the fact that intact bacteria are not present in cloud residuals.

-Fig. 2 and other mass spectra: The two types of particles appear to have no unique ion markers, just differences in the relative ion signals. This makes separating the two particle types out based on their mass spectra rather challenging.

As we already discussed above, it is not surprising that individual mass spectra of all particles in the chamber have nearly the same mass spectral peaks, as shown in the new Figure 3, albeit with different relative intensities. Both aerosolized intact

bacteria and bacteria fragments mixed with agar are composed of similar compounds mixed at different ratios. We have found that the relative fractions of agar and bacterial fragments change with particle size, effecting their mass spectra (Figure 12 of the revised manuscript and the figure above). The distinction between the two particle types is based on *simultaneous* measurements of single particle composition *and* size. As we noted above, particles composed of bacterial fragments mixed with agar that are larger than 700 nm have the same d_{va} and indistinguishable MS from intact bacteria. However, the d_{va} distribution of the intact bacteria has a distinct peak at ~850 nm, while the d_{va} distribution of bacterial fragments mixed with agar does not have a peak in this region.

-Showing the average mass spectra is not that meaningful here. The small but important number fraction of intact bacteria will be obscured by averaging. An estimate of the number fraction of intact bacteria vs. fragments+agar in the different size modes would be really useful.

We already discussed the dependence of particle mass spectra on particle size. Moreover, if intact bacteria were more active than the fragments, they would be enhanced in cloud residuals, resulting in a more prominent larger particle mode in d_{va} size distributions as compared to the clear peak of the intact bacteria mode detected before the expansions.

-9/14: Again, need to know what the CCN/CN fraction was at what max RHw to really evaluate the hygroscopicity of the particles. "very high CCN activation efficiency" is not quantitative.

We have provided the calculated CCN/CN fractions in the revised text and in Table S1. We discussed the issue of RHw above.

-Expansion 3 seems unique in that there is much more ice produced even though the aerosol seems similar to the other expansions, but the reason for this difference is not discussed.

Actually, during Expansion 3 the concentration of ice crystals is lower as described in the text. More ice crystal residuals were sampled and characterized during Expansion 3 because instead of the PCVI, the IS-PCVI was used to select larger cloud particles as described in the text and shown in Figure 13.

-10/14: "Nevertheless, the data presented here show that bacterial fragments mixed with agar preferentially activate as droplets and are the only particles observed in ice residuals." This is essentially the singular conclusion reached from this study, and it is an interesting one. I strongly suggest making this aspect the focus and providing more data and analysis that better supports this conclusion.

We agree, the focus of the paper was to determine which of the two particle types was more CCN and IN active. We have revised the discussion to make that more clear. We have also added the additional data you requested. It is worth noting that in addition to this main point, this manuscript demonstrates the importance of agar on cloud nucleation in laboratory studies, and presents the new finding that particle composition strongly depends on size.

Activation of Intact Bacteria and Bacterial Fragments Mixed with Agar as Cloud Droplets and Ice Crystals in Cloud Chamber Experiments

Kaitlyn J. Suski,[1] David M. Bell,[1] Naruki Hiranuma,[2,3] Ottmar Möhler,[2] Dan Imre,[4] and Alla Zelenyuk[1]

[1]Pacific Northwest National Laboratory, Richland, WA, USA.
[2]Institute of Meteorology and Climate Research – Atmospheric Aerosol Research, Karlsruhe Institute of Technology, Karlsruhe, Germany.
[3]Currently at Department of Life, Earth and Environmental Sciences, West Texas A&M University, Canyon, TX, USA.
[4]Imre Consulting, Richland, WA, USA

Correspondence to: Alla Zelenyuk (alla.zelenyuk-imre@pnnl.gov)

Abstract. Biological particles, including bacteria and bacterial fragments, have been of much interest due to the special ability of some to nucleate ice at modestly ~~low~~ supercooled temperatures. This paper presents results from a recent study conducted on two strains of cultivated bacteria which suggest that bacterial fragments mixed with agar, and not whole bacterial cells, serve as cloud condensation nuclei (CCN). Due to the absence of whole bacteria cells in droplets, they are unable to serve as ice nucleating particles (INPs) in the immersion mode under the experimental conditions. Experiments were conducted at the Aerosol Interaction and Dynamics in the Atmosphere (AIDA) cloud chamber at the Karlsruhe Institute of Technology (KIT) by injecting bacteria-containing aerosol samples into the cloud chamber and inducing cloud formation by expansion over a temperature range of -5 to -12 °C. Cloud droplets and ice crystals were sampled through a pumped counterflow virtual impactor inlet (PCVI) and their residuals were characterized with a single particle mass spectrometer (miniSPLAT). The size distribution of the overall aerosol was bimodal, with a large particle mode composed of intact bacteria and a mode of smaller particles composed of bacterial fragments ~~agar~~ mixed with agar ~~bacterial fragments~~ that were present in higher concentrations. Results from three expansions with two bacterial strains indicate that the cloud droplet residuals had virtually the same size distribution as the smaller particle size mode and had mass spectra that closely matched those of bacterial fragments mixed with agar ~~and bacterial fragments~~. The characterization of ice residuals that were sampled through an ice-selecting PCVI (IS-PCVI) also shows that the same particles that activate to form cloud droplets, bacteria fragments mixed with agar, were the only particle type observed in ice residuals.

1 Introduction

Aerosols affect climate directly, by scattering and absorbing solar and terrestrial radiation and indirectly through interactions with clouds and precipitation (IPCC, 2013). In their role as cloud condensation nuclei (CCN) and ice nucleating particles (INPs), aerosol particles affect cloud microphysical properties (Pruppacher and Klett, 2010). Biological particles, including bacteria, which are found in the atmosphere in various forms but at relatively low number concentrations (Despres et al., 2012),

might play an important role globally as CCN or INPs (Morris et al., 2004;Möhler et al., 2007). While a large body of work on the ice nucleating (IN) activity of biological particles exists, the extent of their role in ice formation within modestly supercooled clouds remains poorly ~~understood~~ constrained ~~(~~(Murray et al., 2012;DeMott and Prenni, 2010;Möhler et al., 2007;Hoose et al., 2010;Spracklen and Heald, 2014;Phillips et al., 2009) ~~and references therein)~~.

Previous studies that looked at the CCN activity of bacteria concluded that bacteria range from very hygroscopic, and hence CCN active under atmospherically relevant conditions (Bauer et al., 2003), to only slightly hygroscopic, activating only at critical supersaturations close to or exceeding those indicating wettability (Franc and DeMott, 1998). It has been suggested, based on contact angle measurements (Sharma and Rao, 2002), that these differences reflect a range of bacteria cell wall types, some of which are hydrophilic, while others are hydrophobic. However, most of these studies utilized aerosolized suspensions of cultured cells that include, in addition to intact bacteria with well-defined cell walls, bacterial fragments mixed with agar growth medium, ~~-~~ in which the bacteria were cultured (Wolf et al., 2015). ~~Particles composed of bacterial fragments mixed with hygroscopic agar are expected to activate into cloud droplets more efficiently than their whole cell counterparts, which are enclosed in a hydrophobic shell. Although i~~It~~'s~~ has been suggested that biological particles may serve as giant CCN (Möhler et al., 2007)~~, in most cases, atmospheric air parcels contain many types of CCN active particles and few biological particles, diminishing the importance of bacteria for liquid cloud activation. In contrast, the fact that~~and because bacterial samples have been shown to induce ice formation at relatively warm temperatures ~~suggestings~~it has been suggested that ~~that~~ they might play an important role as INPs in mixed phase clouds (Möhler et al., 2007).

Depending on the INP composition and size, and on the temperature and relative humidity (RH), ice formation can occur by several pathways. The freezing modes most relevant to bacteria particles are *immersion freezing*, which is induced by a particle immersed in supercooled water ~~(~~(Murray et al., 2012;Vali et al., 2015;Vali et al., 1978) ~~and references therein)~~; *condensation freezing*, in which water condensing on an INP freezes (Pruppacher and Klett, 2010); and *contact freezing* that occurs when a liquid droplet hits an INP and freezes on contact (Cantrell and Heymsfield, 2005). However, for the experiments presented here immersion freezing represents the ~~primary~~ dominant ice formation mechanism (Gallavardin et al., 2008). In immersion freezing, the INP first activates as a liquid cloud droplet, when the RH over water (RH_w) exceeds 100% RH, and subsequently ice forms ~~when this droplet freezes due to the presence of a solid nucleus~~, which means that this ice formation mechanism is tightly connected to the particle CCN activity.

Many biological particle types including pollen (Hader et al., 2014;Augustin et al., 2013;Diehl et al., 2001), fungi (Fröhlich-Nowoisky et al., 2015), and decaying plant material (Schnell and Vali, 1976;Conen et al., 2016) have been identified as efficient INPs. Additionally, IN active macromolecules ~~nano-INPs~~ have been observed from fungi (O'Sullivan et al., 2016), pollen (Pummer et al., 2012), and proteins from IN active bacteria (Wolber et al., 1986). These IN active proteins were shown to be active on their own, in the absence of intact bacteria, demonstrating that a single protein is all that is required to initiate freezing (Govindarajan and Lindow, 1988). Additionally, IN active bacterial fragments have been observed in the ambient environment (Šantl-Temkiv et al., 2015), mineral dust has been observed to be co-located with biological residues ~~,~~ in mixed

phase clouds (Creamean et al., 2013), and IN active proteins from fungi have been shown to attach to dust (O'Sullivan et al., 2016), which can be used as a carrier to transport these biological macromolecules.

Pseudomonas syringae is one bacteria strain that has been shown to nucleate ice at temperatures as high as -2 °C (Maki et al., 1974;Vali et al., 1976). ~~(Vali et al., 1976)~~This bacteria's special ability to nucleate ice at relatively warm temperatures has been shown to cause frost injury to plants (Lindow et al., 1982) leading to decades long speculation that it may play a role in precipitation processes (Vali et al., 1976). A recent study showed that Pseudomonas syringae has a unique structure that orders water at its surface through hydrogen bonding, which allows for efficient latent heat removal, thus enhancing ice formation (Pandey et al., 2016). A store-bought snow inducer, Snomax®, which contains Pseudomonas syringae has been used in laboratory ice nucleation studies. A recent study shows that the ice nucleation ability of Snomax® changes based on sample age and after repeated freeze and thaw cycles (Polen et al., 2016). A different strain of Pseudomonas bacteria, Pseudomonas Fluorescence (PF CGina), that was isolated from glacier melt water in Antarctica was also shown to nucleate ice at warm temperatures (Attard et al., 2012;Amato et al., 2015). Pseudomonas syringae and PF CGina were shown to have decreased viability when exposed to UV light, but only significantly decreased IN activity when exposed to acidic conditions, suggesting that the denaturation of proteins and not cell death has the largest effect on the IN activity of these bacteria (Attard et al., 2012). It was confirmed that cell death does not significantly reduce IN activity of Pseudomonas syringae and PF CGina by Amato et al. (2015).

Several laboratory studies have identified proteins and protein complexes as the ice nucleating entities in Pseudomonas syringae (Lindow et al., 1989;Maki and Willoughby, 1978;Hartmann et al., 2013;Govindarajan and Lindow, 1988). Additionally, 3 protein classes were identified based on their abundance and different ice nucleating abilities (Turner et al., 1990) and it was shown that non-protein compounds that anchor proteins to cell membranes were present in the most IN active classes (Turner et al., 1991). A previous study at the AIDA cloud chamber concluded that both bacterial fragments and whole cells were CCN and IN active, with whole cells being slightly more IN active than the fragments, and the fragments having a higher hygroscopicity than the whole cells (Oehm, 2012). Several other studies have reached similar conclusions ~~indicating~~ that both whole cells and bacterial fragments serve as INPs (Wex et al., 2015;Hartmann et al., 2013;Yankofsky et al., 1981). In contrast, an earlier study at the AIDA chamber suggested that only intact bacteria are IN active (Möhler et al., 2008). The distinction between whole cells and bacterial fragments is important from many perspectives, especially when calculating available surface area, surface site density, and active or frozen fraction of bacteria in laboratory experiments. More importantly, modeling studies suggest biological particles may be an important player in precipitation processes (Burrows et al., 2013;Morris et al., 2004), but because atmospheric concentrations of intact bacteria and bacterial fragments are poorly constrained and expected to be vastly different, it remains uncertain how big of a role bacteria play in mixed phase cloud formation globally.

When interpreting previously published studies, it is important to keep in mind that when a solution containing cultivated bacterial cells is aerosolized, at least two types of particles form: Intact or whole bacterial cells and small particles, composed

of bacterial fragments mixed with agar. The size distribution of the small particle mode depends on the particles generation, i.e. the size of aerosolized droplets, and the concentration of the agar and bacterial fragments in the solution/suspension. Therefore, it would not be surprising to find that its number concentration and size distribution differ from one experimental set-up to the next, and that it could even change with the age of the solution/suspension.

The data presented here were acquired during cloud simulation experiments performed at the AIDA cloud chamber during the first part of the Fifth International Ice Nucleation Workshop (FIN-1). The single particle mass spectrometer, miniSPLAT (Wilson et al., 2015), was utilized to characterize the size and chemical compositions of intact bacteria cells and bacterial fragments mixed with agar before and after cloud formation. Most importantly, it was used to characterize the residuals of liquid droplets and ice crystals formed during the expansions. Cloud particles were separated from interstitial particles with a pumped counterflow virtual impactor (PCVI) or an ice-selecting PCVI (IS-PCVI) (Hiranuma et al., 2016). Comparison between the properties of cloud residuals with the overall particle population in the chamber before and after the expansion allows for the determination of cloud and ice active versus interstitial particles.

As it will be demonstrated below, the results of these measurements, on two different bacteria, indicate that bacterial fragments mixed with agar accounted for the clear majority of particles active as CCN and as INPs, while whole cells activated with much lower probability, if at all.

2 Experimental

The Fifth International Ice Nucleation Workshop (FIN) was a three-part study that aimed to compare a number of single particle mass spectrometers and ice nucleation instruments. The data presented here were collected during FIN-1, which took place in November of 2014 at the AIDA cloud chamber at KIT in Karlsruhe, Germany. Ten single particle mass spectrometers from several research groups around the world were brought together for FIN-1 to simultaneously characterize the size and composition of various types of aerosol particles, including those being used in the AIDA chamber to study their activity as CCN and INPs, Various aerosol types were sampled from the AIDA cloud chamber before, during, and after expansions forming cloud particles and each of these mass spectrometers sampled using their own protocol. The results of the intercomparison will be the subject of future publication. The present manuscript presents the results of measurements, made by miniSPLAT only, during three expansions using two bacteria.

The AIDA cloud chamber and its operation were previously described in detail elsewhere (Möhler et al., 2003). Briefly, the AIDA cloud chamber is an 84 m^3 aluminum vessel in a thermally insulated housing that can be set to a desired ~~relative humidity (~~RH~~)~~, temperature, and pressure. To induce cloud formation, the pressure of the chamber, filled with aerosol particles, is lowered by pumping on the chamber, which causes the gas to expand, the temperature to drop, and the ~~relative humidity (~~RH~~)~~ to increase above ice saturation, depending on the specific experiment. Once supersaturation with respect to water is reached at temperatures below 0°C, cloud droplets, and eventually ice crystals, form. The data presented in this paper are from 3

expansions during the campaign, Expansions 36, 37, and 38, which are referred to as Expansions 1, 2, and 3, respectively, throughout this paper. The mobility size distributions of particles in the AIDA chamber are measured before and after expansions with a scanning mobility particle sizer (SMPS), comprised of a differential mobility analyzer (DMA, TSI Inc., Model 3080) and a condensation particle counter (CPC, TSI Inc., Model 3010). The SMPS sizes particles with mobility diameters larger than 14 nm and smaller than 740 nm, while larger particles, with aerodynamic diameters from 0.5 to 20 µm, are sized with an aerodynamic particle sizer (APS, TSI Inc., Model 3321). Throughout the manuscript the combined SMPS and APS data are shown as volume-equivalent diameters calculated using a particle density of 1.4 g/cm^3 based on previous and measurements (Wex et al., 2015) and optimized assuming a dynamic shape factor of 1 according to Peters et al. (2006). A similar application of volume equivalent diameter in SMPS and APS for use in conjunction with AIDA data can be found in Hiranuma et al. (2015). Total particle number concentrations are measured with a CPC (TSI Inc., Model 3076). Temperature and RH are measured using a number of calibrated sensors (Fahey et al., 2014;Möhler et al., 2003). Optical diameters of cloud droplets and ice crystals are determined using two optical particle counters (welas OPCs, Palas GmbH, sensor series 2300 and 2500). The detection size ranges of the two OPCs, referred to as welas1 and welas2, are ~0.7 to 46 µm and ~5 to 240 µm, respectively (Wagner and Möhler, 2013). The simultaneous use of these two OPCs effectively spans the size range of droplets and ice crystals formed in the chamber. A rough estimate of the number of particles that activated as CCN (CCN/CN) can be calculated by dividing the CPC measured particle concentration prior to the expansion by the maximum value of welas2 measured cloud particles concentrations observed during the expansion. Similarly, a rough estimate of INP/CN can be calculated by dividing the CPC measured concentration before the expansion by the maximum value of Welas2 measured concentrations of cloud particles >larger than 30 µm. These values are provided in Table S1 for each expansion.

A pumped counterflow virtual impactor (PCVI) (Boulter et al., 2006) and an ice-selecting PCVI (IS-PCVI) (Hiranuma et al., 2016) were used to selectively sample cloud droplet and ice crystals, the residuals of which were counted with the CPC and characterized by miniSPLAT and other instruments. PCVIs use a counterflow to reject smaller, interstitial particles, while particles that have enough inertia to pass through the counterflow are transmitted through the inlet. The ratio of the counterflow to the pumped flow changes the inlet cut-size. One advantage of using the PCVI system is to provide residual-laden flows, in which particles are virtually concentrated by a flow concentration factor (i.e., the ratio of input flow to output flow), to the downstream instruments. The IS-PCVI, which has a higher cut-size than other PCVIs (Hiranuma et al., 2016), is intended to be used to reject both interstitial particles and small cloud droplets and allow the larger ice crystals through. The heated evaporation sections installed downstream of each PCVI are maintained at a temperature above 35 °C to evaporate water from the cloud particles leaving the residuals behind. The cut-sizes, enhancement factors, and transmission efficiencies for all of the expansions are given in Table S1. The cut-sizes are based on the measured number of particles transmitted through the PCVI or IS-PCVI and the size distributions of cloud particles in the AIDA chamber. The transmission efficiencies for particles above the cut-size are 94% and 62% Expansions 1 and 2 respectively, respectively, (Gallavardin et al., 2008) and 91.5% for

Expansion 3 (Hiranuma et al., 2016). The fraction of total cloud particles that were transmitted through the PCVI and IS-PCVI (Figure S1) was calculated using Eq. (1), where F_{output} is the CVI output flow (lpm) and F_{input} is the CVI input flow (lpm).

$$Fraction\ of\ the\ droplets\ and\ ice\ crystals\ reached\ at\ the\ CVI(t) = \frac{PCVI\ CPC(t) \times \frac{F_{output}}{F_{input}}}{Welas2(t)} \quad (1)$$

The fraction changes in time due to changing cut-sizes of the inlets and changing size distributions of the activated particles.

Vacuum aerodynamic diameters (d_{va}) and chemical compositions of individual aerosol particles and cloud residuals were measured with miniSPLAT, a single particle mass spectrometer, a detailed description of which is given elsewhere (Wilson et al., 2015). Briefly, individual aerosol particles enter miniSPLAT through an aerodynamic lens inlet (Vaden et al., 2011a) and are detected by light scattering in two optical stages 10.9 cm apart. The time it takes the particles to pass between the two continuous laser beams (532 nm Nd:YAG CrystaLaser, Model CL-300-LO) yields particle velocity, which for a given inlet pressure is related to particle d_{va}. Given that the inlet pressure is changing during the expansions, ~~a pressure dependent size calibration was developed and used.~~ polystyrene latex spheres (PSLs) of known sizes ranging from 73 nm to 993 µm were ~~run~~used to generate a pressure dependent size calibration curve over a range of pressures from 0.9 to 4 Torr. The transmission efficiency through the aerodynamic lens inlet is expected to change by only a few percent with the observed pressure changes during the expansion, as shown in Liu et al. (2007). The dual particle detection is also used to generate a trigger for the excimer laser (GAM Lasers Inc., Model EX-5), operated at 193 nm with a constant laser energy of 1.0 ± 0.1 mJ/pulse, which ablates the particles and generates positive and negative ions.~~The dual particle detection is also used to generate a trigger for the excimer laser (GAM Lasers Inc., Model EX-5), operated at 193 nm with a laser power of ~1.0 ± 0.1 mJ, which ablates the particles and generates positive and negative ions.~~ Single particle mass spectra are obtained with a dual-polarity, z-configuration reflectron time-of-flight mass spectrometer (Z-TOF, Tofwerk AG). miniSPLAT-measured particle number concentrations are calculated by dividing the particle detection rate at the first optical detection stage by the pressure-dependent sampling flow rate as described in detail in Vaden et al. (2011a). All data generated by miniSPLAT are processed, analyzed, and visualized using custom software (Zelenyuk et al., 2008;Zelenyuk et al., 2006).

Suspensions of cultured Pseudomonas syringae and PF CGina 01 were prepared, as described in Hiranuma et al. (2016), by suspending ~10^9 bacteria cells mL^{-1} in sterile water and a small amount of Kings Base Agar. The solutions were atomized using a custom atomizer (Wex et al., 2015), dried by flowing through two diffusion driers (TOPAS, Model DDU 570), and injected into the AIDA chamber prior to expansions.

3 Results and Discussion

3.1 Pseudomonas Syringae Bacteria Characterization

~~Prior to each experiment, t~~The AIDA cloud chamber was preconditioned overnight to reach the desired experimental temperature. Before ~~the 1st expansion presented here (Expansion 1),~~the expansions a suspension of ~~Pseudomonas syringae~~ bacteria (Pseudomonas syringae for expansion 1 and PF CGina for expansions 2 and 3) was aerosolized, dried, and the resulting particles were introduced into the chamber. Figure 1 shows the calculated volume equivalent diameter (d_{ve}) size distributions of particles present in AIDA before ~~the~~ expansion 1, which was obtained by combining measurements by the SMPS (black line) and the APS (red line). ~~Figure 1a shows a~~The size distribution is bimodal with a smaller size mode that peaks at ~70 nm and a broad peak at ~800 nm. The miniSPLAT-measured vacuum aerodynamic size (d_{va}) distribution, shown in Figure 1b, is also ~~has two distinct peaks at~~bimodal with modes at 180 nm and ~850 nm~~, for the small and large size modes, respectively~~. The difference between the small particle peak positions of the measured d_{va} and d_{ve} size distributions is due to particle density ($\rho > 1$ g cm^{-3}) and the miniSPLAT's small particle detection limit (50% cut off at 85 nm, marked with a green line in Figure 1a) (Vaden et al., 2011b). This type of bimodal size distribution has been observed previously with other aerosolized suspensions of cultivated bacteria (Wex et al., 2015;Wolf et al., 2015;Möhler et al., 2008). The large size mode corresponds to intact/whole bacteria cells and the smaller mode is composed of bacterial fragments mixed with agar.

Representative positive and negative ion mass spectra (MS) of the two particle modes are shown in Figure 2. The reference MS of the small particle mode includes MS of particles smaller than 300 nm and that of the large particle mode/intact bacteria includes the MS of particles larger than 700 nm. Comparison between the reference MS of the two particle modes shows that nearly all the peaks are present in the MS of both modes. However, the positive ion MS of the two modes exhibit significantly different relative peak intensities, while the negative ion MS are very similar. The positive ion MS indicate the presence of many organics and metal ions, including carbon containing fragments ($^{12}C^+$, $^{15}CH_3^+$, $^{28}CO^+$), $^{41}CH_3CO^+$, $^{44}CO_2/CH_3COH^+$), ammonia ($^{18}NH_3^+$), organic nitrogen ($^{28}HCNH^+$, $^{30}H_2NCH_2^+$, $^{70}HNCH(CH_2)_3^+$, $^{85}C_5NH_{10}^+$) sodium ($^{23}Na^+$), potassium ($^{39/41}K^+$), calcium ($^{40}Ca^+$), and calcium oxides ($^{56}CaO^+$, $^{113}(CaO)_2H^+$). The negative ion MS show the presence of organic nitrogen ($^{26}CN^-$, $^{42}CNO^-$), chloride ($^{35/37}Cl^-$), organics ($^{45}HCO_2^-$, $^{50}C_3N^-$, $^{71}C_3H_3O_2^-$), and phosphates ($^{63}PO_2^-$, $^{79}PO_3^-$, $^{97}H_2PO_4^-$). The ions were identified via comparison to previous studies on bacteria (Pratt et al., 2009;Zawadowicz et al., 2017;Wolf et al., 2015;Fergenson et al., 2004;Srivastava et al., 2005;Czerwieniec et al., 2005). The positive ion MS for intact cells show ~~relatively lower intensities for the metal ions ($^{23}Na^+$, $^{39/41}K^+$, $^{40}Ca^+$) and~~ significantly higher intensities for the organic peaks ($^{12}C^+$, $^{15}CH_3^+$, $^{18}NH_3^+$, $^{28}CO/HCNH^+$, $^{30}H_2NCH_2^+$, $^{44}CO_2/CH_3COH^+$, $^{70}HNCH(CH_2)_3^+$, $^{85}C_5NH_{10}^+$) as compared to those of the small particle mode, which are dominated by the potassium peak. The same MS are presented in Figure ~~S1~~ 3 in expanded scale together with the MS of pure agar particles. Comparison between MS of agar and the small particle mode shows their positive ion MS ~~to be nearly identical~~have the same peaks just with varying ion intensities and the absence of ~~an unidentified~~ peak at m/z 131 (possibly, $C_7H_{17}NO$) in the agar. ~~, while T~~the agar negative ion MS ~~are significantly different, with the agar MS containing no~~ have sulfate peaks ($^{64}SO_2^-$), $^{81}HSO_3^-$, $^{97}HSO_4^-$) and lack some organic ions ($^{45}HCO_2^-$, $^{71}C_3H_3O_2^-$) as compared to the bacteria MS. ~~-~~The size distributions and MS provide direct evidence that the smaller particles are composed of ~~agar *mixed* with~~ bacterial fragments mixed with agar, while the larger size particle mode corresponds to intact bacteria cells. The MS of

intact bacteria shown in Figures 2 and 3~~S1~~ are similar to previously published single particle mass spectra of laboratory-generated Pseudomonas syringae acquired by two other single particle mass spectrometers (Pratt et al., 2009;Zawadowicz et al., 2017). The negative ion MS presented here and in previous studies are virtually the same, while the positive ion MS presented in this study exhibit significantly higher intensity in organic peaks, most likely due to the differences in the ablation laser power or wavelength (266 nm in Pratt et al. (2009) and 193 nm in this study and Zawadowicz et al. (2017)). Moreover, these studies do not mention the presence of two particle size modes nor distinguish between their mass spectra.~~The negative ion MS are virtually the same, while the positive ion MS presented here exhibit significantly higher intensity in organic peaks, most likely due to the differences in the ablation laser wavelength Zawadowicz et al. (2017) or power. Moreover, these studies do not mention the presence of two particle size modes~~.

The size distributions shown in Figure 1a indicate a total number concentration of particles in the chamber of ~2,500 particles cm^{-3}~~, ~1,000 particles cm^{-3} of which are larger than 100 nm,~~ and ~~only~~ ~100 particles cm^{-3}, or 4%, are intact bacteria. In comparison, the d_{va} size distribution (Figure 1b) yields 7% for the fraction of intact bacteria, since more than half of the particles in the smaller size mode are too small to be detected by miniSPLAT. It is important to point out that the size, number concentration, and the relative fraction of the small particles containing bacterial fragments can vary from experiment to experiment and ~~that they~~ are determined by the solution/suspension concentrations of agar, intact bacteria, and cell fragments, as well as how the bacteria culture is grown and prepared ~~for the experiment~~ (Wolf et al., 2015), and ~~could~~ may~~even~~ change with the age of the solution/suspension. ~~Given the differences in dry size, composition, and hygroscopicity of these two particle types, they might be expected to have different cloud droplet and ice nucleation activities.~~

3.2 Cloud Formation and Cloud Droplet Characterization

Cloud formation ~~is~~ was induced by lowering the pressure in the AIDA chamber, using active pumping, which ~~lowers~~ lowered the ~~pressure and~~ temperature ~~of the gas in the chamber~~ and increase~~s~~d the ~~results in an increase in~~ RH, ~~which is~~ shown in Figure 4~~3~~a. As the chamber became supersaturated with respect to both ice and water, cloud droplets and ice crystals formed, which is illustrated in Figure 3b with a false color plot of the welas2-measured size distribution as a function of expansion time. ~~As the temperature decreased and the RH increased, the number concentrations of droplets larger than 5 µm rapidly increased.~~ The number concentration of cloud droplets and ice crystals (particles larger than 5 µm, plotted as a black line) quickly reached ~900 particle cm^{-3} and then decreased slowly to 400 particles cm^{-3}. An estimate of the fraction of particles that activated as cloud droplets (CCN/CN) yields 0.45, indicating that less than half of the particles were incorporated into droplets. After ~500 sec, as pumping stopped, the temperature increased, RH dropped, and the droplet number concentration decreased mainly due to water evaporation. During the expansion, the vast majority of the droplets remained smaller than 14 µm. The few ice crystals that formed are apparent in the figure as a second mode of much larger particles (marked in Figure 4~~3~~b) mainly visible at ~100 to 200 sec, after which point their numbers rapidly decreased mainly because of settling losses.

~~The welas2 data are also plotted in Figure 3c in a 2D plot format. The figure shows that the number concentration of cloud droplets and ice crystals (particles larger than 5 µm, plotted as a black line) quickly reaches ~900 particle cm^{-3} and then decreases slowly to 400 particles cm^{-3}, before it rapidly drops to zero.~~ Ice crystal concentrations derived from welas2-measured number concentrations of particles larger than 30 µm ~~are indicated by the (~~pink line in Figure 43c)~~. Ice crystals appear later in the expansion, and their numbers~~ reach a maximum of 3 particles cm^{-3}, or more than 200 times lower than droplets. An estimate of the fraction of particles that were incorporated into ice crystals ~~.~~ shows that INP/CN ≈ 0.0014. ~~As a reminder, before the expansion, there were ~ 2,500 particles cm^{-3} in the chamber, including only ~100 intact bacteria cm^{-3}. Early in the expansion when there were mostly droplets present in the chamber, the number of cloud particles reached 900 particles cm^{-3}, signifying a very high CCN activation efficiency of particles composed of bacterial fragments mixed with agar.~~

~~The CPC and miniSPLAT measured number concentrations of cloud residuals transmitted through the PCVI, shown in Figure 3c in yellow and green, respectively, exhibit very similar behavior. These data indicate a rapid increase early in the expansion and a relatively fast drop to zero after ~250 sec, with the temporal evolution of the two independently measured residuals number concentrations showing good agreement.~~ Figures 43b and 43c show that during Expansion 1 the PCVI transmitted predominantly droplets, the residuals of which were characterized by the CPC and miniSPLAT.

The d_{va} size distribution of cloud residuals (Figure 5) is virtually the same ~~measured by miniSPLAT is presented together with the d_{va} size distribution of the~~ as the size distribution of particles in the chamber before the expansion except that ~~in Figure 4~~. ~~The miniSPLAT measured size distribution of particles composed of agar and bacterial fragments before the expansion and of cloud residuals are virtually the same, and~~ the intact bacteria, i.e. the large particle mode, is "missing" from the size distribution of the cloud residuals. ~~These data provide direct evidence that under the experimental conditions in Expansion 1, particles composed of bacterial fragments mixed with agar preferentially activated to form cloud droplets, a small fraction of which became ice crystals, as illustrated in Figure 3~~.

In addition to the d_{va} size distribution, miniSPLAT measured positive and negative ion MS of individual cloud residuals, which are presented in Figure 65 superimposed on the reference MS of intact bacteria (large mode particles) (Figure 65a and b) and on the reference MS of the small particle mode composed of agar and bacterial fragments (Figure 65c and d) measured before the expansion. Comparison between the three particle types shows that the intact bacteria have higher relative intensities of many organic and nitrogen-containing ($^{15}CH_3^+$, $^{18}NH_3^+$, $^{28}HCNH^+$, $^{30}H_2NCH_2^+$, $^{44}CO_2^+$, $^{70}HNCH(CH_2)_3^+$, $^{85}C_5NH_{10}^+$) and calcium ions ($^{40}Ca^+$, $^{56}CaO^+$) than the cloud residuals, but the small particle mode ~~cloud residuals have~~has nearly the same MS as the cloud residuals~~that plotted in Figure 2a for the small particle mode in the chamber before the expansion.~~ ~~. This suggests that the bacteria fragments mixed with agar are serving as CCN, which is consistent with the conclusions based on the measured d_{va} size distributions.~~ The small differences between the MS of residuals and the small particle mode suggest a slightly higher content of organics in the residuals, indicated by higher relative intensities of $^{28}HCNH^+$, $^{30}H_2NCH_2^+$, and $^{44}CO_2^+$, which is due to the fact that the MS of residuals includes all detected particles, while the reference MS of the small particle mode includes only particles smaller than 300 nm. These MS differences will be further examined below in a detailed analysis of data obtained

during Expansion 2, where the observed differences are larger and, therefore, easier to analyze. Taken together with the size distributions, these data provide direct evidence that under these experimental conditions, from the two particle types present in the chamber, particles composed of bacterial fragments mixed with agar preferentially activated to form cloud droplets.

~~In summary, prior to Expansion 1 there were ~2,500 particles cm^{-3} in the chamber, ~10% of which were intact bacteria. During the expansion, the maximum number of droplets formed reached 900 particles cm^{-3}, and the average droplet concentration was 650 particles cm^{-3}, while the maximum ice crystal concentration was 3 particles cm^{-3} and the average was slightly less than 1 crystal cm^{-3}. As a result, the clear majority of the particles transmitted through the PCVI were droplets. The miniSPLAT-measured d_{va} size distribution of the cloud residuals is nearly identical to that of the small particle mode. Consistent with the size distribution, the MS of the cloud residuals is nearly the same as the reference MS of the small particle mode, demonstrating preferential droplet activation of smaller particles composed of bacterial fragments mixed with agar, as well as, the absence of intact cells in droplets residuals.~~

3.3 PF CGina Bacteria and Cloud Droplet Characterization

Expansion 2 was performed in the same ~~exact~~ manner as Expansion 1, except that ~~a~~ different bacteria, ~~cultivated~~ PF CGina~~01~~, was used. Figure 7~~6~~a presents the size distributions of particles in the chamber prior to Expansion 2, showing two particle modes, the small size mode, composed of agar and bacterial fragments, which peaks at d_{ve}≈60 nm, and the intact bacteria, which peaks at d_{ve}≈700 nm. There were 1,800 particles cm^{-3}, ~4% of which were intact bacteria. Similarly, the d_{va} size distribution, shown in Figure ~~6b~~7b~~,~~ ~~indicates two particle modes: the~~shows the small ~~size~~ particle mode peaking at d_{va}≈160 nm, composed of agar and bacterial fragments~~-~~, and the intact bacteria mode, which peaks at d_{va}≈850 nm and represents ~9% of particles detected and sized ~~by miniSPLAT~~ prior to Expansion 2. Comparison between the reference MS of the two particle modes present before Expansion 2 is presented in Figure 8~~7~~, where the small mode includes particles smaller than 300 nm, and the large mode represents particles larger than 700 nm. As in the case of Expansion 1, the MS show that the small particles are composed of agar and bacterial fragments~~, as evident by the presence of phosphate peaks in the negative ion MS~~. The difference between the two positive ion reference MS for PF CGina~~01~~ are~~is~~ very similar to the pattern observed for Pseudomonas syringae bacteria (Figure 2) and contain all of the same ions.

The temporal evolution of pressure, temperature, and RH during Expansion 2 are shown in Figure 9~~8~~a. The welas2-measured size distributions of cloud particles ~~as a function of time, shown in~~(~~-~~Figure 9~~8~~b) ~~as a false color image,~~ reveal that most of the activated particles were liquid droplets smaller than 10 µm, and ~~that~~ only a small number of cloud particles were ice crystals~~. , as determined by their significantly larger optical diameters. The analysis of the welas2-measured number concentrations of cloud droplets and ice crystals as a function of time presented in Figure 8c indicates that t~~The average droplet and ice crystal concentrations (Figure 9c) were ~730 particles cm^{-3} and ~1 particle cm^{-3}, respectively, with ice crystal peak concentrations reaching ~3 particles cm^{-3} at 150 to 250 seconds from the start of the expansion. As a result, particles transmitted through the PCVI to the CPC and miniSPLAT during Expansion 2 were predominantly liquid droplets. The CPC- and miniSPLAT-

measured number concentrations of particles transmitted by the PCVI, ~~also presented in~~ Figure ~~9~~8c, show rapid increases early in the expansion and slower decreases thereafter, displaying the same behavior as in Expansion 1. A lower percentage of particles were activated into droplets (30 %) than in the first expansion, but roughly the same percentage were activated into ice crystals (0.16%).

The miniSPLAT-measured d_{va} distributions of cloud residuals (blue) and particles in the chamber prior to the expansion (green) are shown in Figure 10~~9~~. As with Expansion 1, the d_{va} distribution of cloud residuals is nearly identical to that of the small particle mode present in the chamber before the expansion. An expanded scale of the intact bacteria size region, shown in the figure inset, indicates no detectable intact bacteria in cloud residuals.

The average positive ion MS of cloud residuals is shown in Figure 11~~0~~. For comparison, it is superimposed on the reference MS of the small particle mode (Figure 11~~0~~a) and intact bacteria (Figure 11~~0~~b). The MS of residuals shows that they contain slightly more organics ($^{12}C^+$, $^{15}CH_3^+$, $^{28}HCNH^+$, $^{30}H_2NCH_2^+$, $^{44}CO_2^+$, $^{70}HNCH(CH_2)_3^+$, $^{85}C_5NH_{10}^+$) than the particles that were included in the reference MS of the small particle mode. It is important, however, to note that the residual MS includes all particles, while the reference MS contains only particles smaller than 300 nm. A possible explanation for the observed difference between the two MS is that the organic content of the small particle mode increases with particle size, i.e. larger particles contain more or larger bacterial fragments and~~, hence,~~ relatively less agar. Indeed, Figure 12~~1~~ shows that the fraction of characteristic organic peaks (m/z 28 and 44) s ~~(peaks at *m/z* ≥ 44, 70, 85)~~ relative to K^+, which serves as a simple qualitative measure of the relative fraction of bacterial fragments and agar in these particles, is increasing with particle size. The figure includes ~~(in dashed line)~~ the d_{va} distribution of cloud residuals (via a dashed line) for reference. ~~As a reminder, a schematic representation of the measured d_{va} size distribution of cloud residuals, is shown in dashed blue line.~~ For comparison, the same analysis ~~applied to the MS of pure agar and intact bacteria particles yields~~shows that the K^+ peak contributes 86% of the mass spectral ~~area~~intensity for pure agar and ~~and~~ 13% for intact bacteria~~for the K^+ MS peak, respectively~~. To examine this further, we compare in Figure S2a the MS of cloud residuals smaller than 300 nm ~~were separated out, shown in~~to ~~(Figure S2a), and are nearly identical to~~ the reference MS of the small particle mode measured before the expansion and find them to be ~~,~~nearly identical. This indicates that they are bacterial fragments mixed with agar. The MS of cloud residuals that are larger than 300 nm have greater ion intensities for the organic peaks ($^{28}CO/HNCH^+$, $^{44}CO_2/CH_3COH^+$, $^{70}HNCH(CH_2)_3^+$, $^{85}C_5NH_{10}^+$) than the bacterial fragments mixed with agar, but slightly smaller ion intensities than those of the reference MS of intact bacteria, as shown in Figure S2b. These differences in ion intensities are not sufficient to eliminate the possibility that some of the larger cloud residuals could be smaller intact bacteria.~~, i.e. bacterial fragment mixed with agar particles smaller than 300 nm, while the MS of cloud residuals that are larger than 300 nm, which in this expansion were dominated by particles whose d_{va} is ~500 nm, is similar~~higherpeak, but not exactly the same, than the small particles but lower peak as the reference MS of intact bacteria, as shown in Figure S2b~~for same peaks (Figure S2b). These small differences MS peak~~are not sufficient to eliminate the possibility that some of the cloud larger activated cloud residual larger particles are in fact small intact bacteria.~~

Overall, the d_{va} size distributions and MS of cloud residuals are like those of the small particle mode, although the larger residuals, which contain more organics, could be smaller intact bacteria. Nevertheless, t~~T~~he data clearly show that the ~~vast~~ intact bacteria contribute~~make~~ a significantly lower fraction, if a~~ny~~t all, to ~~of majority of intact bacteria in the chamber did not activate~~the cloud residuals ~~were bacteria fragments~~than they contribute to the total particle population present before the expansion. In all respects, the miniSPLAT data for PF CGina01 are consistent with those for Pseudomonas syringae (Expansion 1) and confirm the preferential droplet activation of particles composed of ~~agar mixed with~~ bacterial fragments mixed with agar compared to ~~with~~ intact bacteria.

3.4 PF CGina Ice Crystal and Droplet Characterization

Expansion 3 followed the same pumping strategy and expansion temperatures as the previous expansions, but was conducted on the PF CGina particles which remained in the AIDA chamber after Expansion 2. The d_{ve} size distributions of these particles, shown in Figure 7~~6~~a as dashed lines, are nearly identical to those measured before Expansion 2, despite a decrease in the total particle number concentration. During Expansion 3, the cloud residual particles, sampled by the CPC and miniSPLAT, were transmitted through ~~the~~ a different inlet, the IS-PCVI, in order to reduce the number of droplets transmitted to allow for characterization of ice crystal residuals.

Changes in chamber pressure, temperature, and RH for Expansion 3 are shown in Figure 13~~2~~a. A false color plot of the activated particles size distribution measured by welas2, as a function of time, is presented in Figure 13~~2~~b. Figure 13~~2~~c displays the welas2-measured total number of activated particles as a function of time (black), which ~~almost~~ reaches a maximum of ~700 particles cm^{-3}~~.~~, Before the expansion, 1456 cm^{-3} particles were present in the chamber indicating that 47% of the particles activated as CCN~~a very high CCN activation efficiency~~. In addition, it shows the number concentrations of cloud particles with optical diameters larger than 15 µm but smaller than 20 µm (light blue) and the number of particles larger than 20 µm (pink). The former may correspond to the number of droplets transmitted by the IS-PCVI, while the latter may be relevant to transmitted ice crystals. Comparison between the two shows that the IS-PCVI transmitted nearly equal numbers of ice crystals and droplets to miniSPLAT and the CPC. A small percentage of particles (0.04%) formed ice crystals. miniSPLAT and the CPC-measured particle number concentrations are also shown in Figure 13~~2~~c. Both instruments show a rapid rise in the concentration of cloud residuals, followed by a significant drop in concentration with time. Early in the expansion, most of the transmitted particles are droplets, but later, between 302 and 557 seconds after the expansion started, the number of droplets and ice crystal residuals becomes comparable, as shown in Figure 13~~2~~c.

Two particle modes are present in the d_{va} size distribution of particles in the chamber before Expansion 3 (Figure 13~~4~~, green trace). Figure 14~~3~~ also shows the d_{va} size distributions of all cloud residuals detected throughout the expansion (blue) and cloud residuals detected late in the expansion (302-557 seconds, light blue), when the number concentration of droplets and ice crystals were approximately equal ~~(light blue)~~. Both cloud residual size distributions are nearly the same as that of the small particle mode and show no distinct peak in the size region of intact bacteria.

The average MS of particles sampled through the IS-PCVI throughout the expansion and later in the expansion are shown in Figure 1~~4~~5. The fact that the two MS are virtually identical suggests that the compositions of particles that remain as droplets and those that activate into ice crystals are not different, which is consistent with the finding that the size distributions are the same.

The residual size distributions and compositions combined again confirm that the majority of particles that served as CCN and INPs were bacterial fragments mixed with agar. While there is no clear indication that intact bacterial cells were activated, it cannot be ruled out that larger cloud residuals were small intact bacteria mixed with agar.

These results are consistent with previous studies that show that whole cells are not necessary for ice formation because IN active proteins and protein complexes can serve as INPs (Lindow et al., 1989;Maki and Willoughby, 1978;Hartmann et al., 2013;Govindarajan and Lindow, 1988). However, it has generally been assumed that whole cells will also nucleate ice (Möhler et al., 2008;Wex et al., 2015;Lindow et al., 1989) and are more active than a single IN active protein (Govindarajan and Lindow, 1988) or bacterial fragment (Yankofsky et al., 1981;Hartmann et al., 2013). The ~~suggestion~~ explanation for enhanced IN activity of intact bacteria is that IN active proteins collect in the cell membrane (Lindow et al., 1989;Govindarajan and Lindow, 1988) and become concentrated on the surface of intact cells thus enhancing their IN activity ~~of intact bacteria~~. ~~Nevertheless~~However, the data presented here show that bacterial fragments mixed with agar preferentially activate as droplets and are the only particles observed in ice residuals under these experimental conditions.

4 Conclusions and Implications for Future Studies

This paper presents the results of measurements of particle number concentrations, size distributions, and compositions of aerosol particles produced from two types of bacteria particles in the AIDA chamber for three separate expansions, before and after the expansions. In all cases, the data show the presence of two distinct particle types in the chamber: particles larger than ~ 700 nm that are intact bacteria, and small particles, with a d_{ve} distribution that peaks at ~65 nm, that are composed of ~~agar mixed with~~ bacterial fragments mixed with agar. The MS show that the small and large particles have distinct MS, representing differences in particle compositions. The small particles are composed of a mixture of bacterial fragments and agar, as determined by comparison with the MS of pure agar particles and intact bacteria. In addition, a detailed analysis of the MS of all particles shows that the organic content of particles relative to potassium increases with particle size, indicating that smaller particles ~~are dominated~~have a larger ~~contribution~~fraction of ~~by~~ agar, whereas larger particles have more organics, i.e. bacterial fragments ~~and/or bacterial cells~~.

The concentration of small particles in the chamber was about thirty times higher than that of intact bacteria for all expansions. The two particle modes in the chamber were detected before and after ~~the~~ three expansions, providing direct evidence that intact bacteria remain intact throughout the expansion and do not burst upon freezing or drying.

In the three expansions presented here, cloud activation occurred between –5 and -12 °C to form cloud droplets, a small fraction of which froze into ice crystals (0.0004-0.0016). ~~The cloud droplets had a wide size distribution of optical diameters that peaked at about 8 µm with some being as large as 15 µm. Ice crystals had a very wide size distribution with some having optical diameters as large as 200 µm.~~ Cloud droplet concentrations were ~~~30-47% of the total particle number concentration in the AIDA chamber, which is significantly higher than the concentration of intact bacteria (4%).

The cloud particles were separated with the PCVI or IS-PCVI, and their residuals were characterized with miniSPLAT. The data in all three expansions present virtually the same picture. The d_{va} size distributions of cloud residuals were devoid of the large particle/ intact bacteria mode and were nearly the same as the miniSPLAT-measured d_{va} distributions of the small particle/ bacterial fragment mode acquired before and after the expansions, providing direct evidence that bacterial fragments mixed with agar ~~most of the particles that~~ activated to form either droplets or ice crystals were ~~bacterial fragments mixed with agar~~ with much higher efficiency than intact bacteria. ~~The similarity between the d_{va} distributions of the small particle mode and the cloud residuals is consistent with the relatively high droplet activation probability and the fact that on the small particle side the d_{va} distribution is determined by the instrument detection limit.~~

MS analysis of the cloud residuals confirms that, while both intact bacterial cells and bacterial fragments mixed with agar were present in the AIDA chamber before and after the expansions, the latter represented a much larger fraction of particles that served as CCN and as INPs than present in the chamber~~.~~, which is consistent with the d_{va} size distributions of cloud residuals. These results were replicated in three expansions, for two different bacteria strains, Pseudomonas syringae and PF CGina 01, suggesting that this behavior may be representative of bacteria in general, or at least of cultivated bacteria used in most laboratory experiments. This is the first study to characterize ~~at~~ the size distributions and mass spectra of bacteria cloud residuals sampled from the AIDA chamber. The detailed size distributions downstream of the PCVI and IS-PCVI enabled identification of the particle types in the AIDA chamber that were activated into cloud droplet and ice crystals.

It is important to note that at the activation temperatures and RH_w~~s~~ of the three expansions presented here, particles first activate as CCN to form cloud droplets and ice crystals form by immersion freezing. If the reports suggesting that some strains of intact bacteria are ~~not~~ weakly hygroscopic (Franc and DeMott, 1998;Sharma and Rao, 2002) are correct, it is not surprising to find that intact bacteria have limited CCN activity, and by necessity, a negligible amount can serve as INP in the immersion mode. Drop freezing and other bulk immersion freezing techniques bypass the issue of limited hygroscopicity by submerging whole cells in a droplet or well of water, artificially overcoming the barrier of CCN activation. These distinctions are important to consider when relating laboratory INP measurements to estimations of ice formation in atmospheric clouds. A recent modeling study has shown that competition for water vapor can inhibit ice formation in clouds due to the most CCN-active particles taking up all the water and leaving the more IN active, but less CCN active, particles as interstitial aerosol and thus, unable to form ice in clouds (Simpson et al., 2017). The study presented here shows that, in contrast to intact bacteria, particles composed of bacterial fragments mixed with agar are CCN active and a fraction of their resulting cloud droplets freeze to make ice crystals. There was possibly competition for water vapor in these expansions as only ~30-47% of particles formed droplets.

Therefore, the most hygroscopic particles would be the ones to activate as CCN. ~~While agar is hygroscopic, pure agar particles do not freeze to form ice crystals at the temperature range examined in this study(Hiranuma and Möhler, 2018), indicating that the bacterial fragments served as INPs in these expansions.~~

If agar ~~is essential to~~aids in transforming bacterial fragments into effective CCN and INP by enhancing their hygroscopicity, ~~as the data presented here suggest,~~ then ~~in the ambient atmosphere bacterial fragments might not be IN active unless mixed with hygroscopic substances that can enhance the CCN activity. Thus,~~ it is important to quantify the role agar plays in CCN and IN activity of bacteria by conducting experiments on bacterial samples that do not contain ~~no~~ agar. Pure agar particles do not freeze to form ice crystals at the temperature range examined in this study (Hiranuma and Möhler, 2018), indicating that the bacterial fragments served as INPs in these expansions even if the agar enhanced their hygroscopicity. Most laboratory studies on bacteria use cultivated bacteria to make measurements that are then extrapolated to atmospheric conditions. However, these measurements may not accurately reflect the CCN or IN activity of non-cultured bacteria under atmospheric conditions.~~Similarly, it is important to investigate the effect of atmospherically relevant hygroscopic compounds, like sulfates and nitrates, which could coat bacterial fragments suspended in the atmosphere transforming them into CCN and IN active particles.~~

Data availability. The data used in this manuscript are available at https://dtn2.pnl.gov/data/release/2018_Suski_et_al_Bacteria_Paper/.

Competing interests. The authors have no conflict of interest.

Special issue statement. This article is part of the special issue “Fifth International Workshop on Ice Nucleation (FIN)”. It is not associated with a conference.

Acknowledgments. Support for AZ, DMB, and KS was provided by the U.S. Department of Energy (DOE) Office of Biological and Environmental Research (OBER) Atmospheric Research Systems Program (ASR). Development of miniSPLAT was funded by the DOE Office of Science, Office of Basic Energy Sciences, Division of Chemical Sciences, Geosciences & Biosciences and EMSL User Facility sponsored by the DOE OBER and located at Pacific Northwest National Laboratory. The valuable contributions of the FIN organizers, their institutions, and the FIN-1 Workshop science team are also gratefully acknowledged. OM and NH thank the Engineering and Infrastructure group members at KIT IMK-AAF (Georg Scheurig, Tomasz Chudy, Rainer Buschbacher, Olga Dombrowski, Steffen Vogt, Jens Nadolny and Frank Schwarz) for their technical support during FIN-1. The AIDA work was partly funded by the Helmholtz Association through its research programme 'Atmosphere and Climate (ATMO)'.

References

Amato, P., Joly, M., Schaupp, C., Attard, E., Mohler, O., Morris, C. E., Brunet, Y., and Delort, A. M.: Survival and ice nucleation activity of bacteria as aerosols in a cloud simulation chamber, Atmos Chem Phys, 15, 6455-6465, 2015.

Attard, E., Yang, H., Delort, A. M., Amato, P., Poschl, U., Glaux, C., Koop, T., and Morris, C. E.: Effects of atmospheric conditions on ice nucleation activity of Pseudomonas, Atmos Chem Phys, 12, 10667-10677, 2012.

Augustin, S., Wex, H., Niedermeier, D., Pummer, B., Grothe, H., Hartmann, S., Tomsche, L., Clauss, T., Voigtländer, J., Ignatius, K., and Stratmann, F.: Immersion freezing of birch pollen washing water, Atmos. Chem. Phys., 13, 10989-11003, 10.5194/acp-13-10989-2013, 2013.

Bauer, H., Giebl, H., Hitzenberger, R., Kasper-Giebl, A., Reischl, G., Zibuschka, F., and Puxbaum, H.: Airborne bacteria as cloud condensation nuclei, J Geophys Res-Atmos, 108, 10.1029/2003jd003545, 2003.

Boulter, J. E., Cziczo, D. J., Middlebrook, A. M., Thomson, D. S., and Murphy, D. M.: Design and performance of a pumped counterflow virtual impactor, Aerosol Sci Tech, 40, 969-976, 10.1080/02786820600840984, 2006.

Burrows, S. M., Hoose, C., Poschl, U., and Lawrence, M. G.: Ice nuclei in marine air: biogenic particles or dust?, Atmos Chem Phys, 13, 245-267, DOI 10.5194/acp-13-245-2013, 2013.

Cantrell, W., and Heymsfield, A.: Production of ice in tropospheric clouds - A review, B Am Meteorol Soc, 86, 795-807, 2005.

Conen, F., Stopelli, E., and Zimmermann, L.: Clues that decaying leaves enrich Arctic air with ice nucleating particles, Atmospheric Environment, 129, 91-94, http://dx.doi.org/10.1016/j.atmosenv.2016.01.027, 2016.

Creamean, J. M., Suski, K. J., Rosenfeld, D., Cazorla, A., DeMott, P. J., Sullivan, R. C., White, A. B., Ralph, F. M., Minnis, P., Comstock, J. M., Tomlinson, J. M., and Prather, K. A.: Dust and Biological Aerosols from the Sahara and Asia Influence Precipitation in the Western U.S., Science, 339, 1572-1578, 2013.

Czerwieniec, G. A., Russell, S. C., Tobias, H. J., Pitesky, M. E., Fergenson, D. P., Steele, P., Srivastava, A., Horn, J. M., Frank, M., Gard, E. E., and Lebrilla, C. B.: Stable isotope labeling of entire Bacillus atrophaeus spores and vegetative cells using bioaerosol mass spectrometry, Anal Chem, 77, 1081-1087, 10.1021/ac0488098, 2005.

DeMott, P. J., and Prenni, A. J.: New Directions: Need for defining the numbers and sources of biological aerosols acting as ice nuclei, Atmospheric Environment, 44, 1944-1945, 2010.

Despres, V. R., Huffman, J. A., Burrows, S. M., Hoose, C., Safatov, A. S., Buryak, G., Frohlich-Nowoisky, J., Elbert, W., Andreae, M. O., Poschl, U., and Jaenicke, R.: Primary biological aerosol particles in the atmosphere: a review, Tellus B, 64, 2012.

Diehl, K., Quick, C., Matthias-Maser, S., Mitra, S. K., and Jaenicke, R.: The ice nucleating ability of pollen - Part I: Laboratory studies in deposition and condensation freezing modes, Atmos Res, 58, 75-87, 2001.

Fahey, D. W., Gao, R. S., Möhler, O., Saathoff, H., Schiller, C., Ebert, V., Kramer, M., Peter, T., Amarouche, N., Avallone, L. M., Bauer, R., Bozoki, Z., Christensen, L. E., Davis, S. M., Durry, G., Dyroff, C., Herman, R. L., Hunsmann, S., Khaykin, S. M., Mackrodt, P., Meyer, J., Smith, J. B., Spelten, N., Troy, R. F., Vomel, H., Wagner, S., and Wienhold, F. G.: The AquaVIT-1 intercomparison of atmospheric water vapor measurement techniques, Atmos Meas Tech, 7, 3177-3213, 2014.

Fergenson, D. P., Pitesky, M. E., Tobias, H. J., Steele, P. T., Czerwieniec, G. A., Russell, S. C., Lebrilla, C. B., Horn, J. M., Coffee, K. R., Srivastava, A., Pillai, S. P., Shih, M. T. P., Hall, H. L., Ramponi, A. J., Chang, J. T., Langlois, R. G., Estacio, P. L., Hadley, R. T., Frank, M., and Gard, E. E.: Reagentless detection and classification of individual bioaerosol particles in seconds, Anal Chem, 76, 373-378, 2004.

Franc, G. D., and DeMott, P. J.: Cloud activation characteristics of airborne Erwinia carotovora cells, J Appl Meteorol, 37, 1293-1300, Doi 10.1175/1520-0450(1998)037<1293:Cacoae>2.0.Co;2, 1998.

Fröhlich-Nowoisky, J., Hill, T. C. J., Pummer, B. G., Yordanova, P., Franc, G. D., and Pöschl, U.: Ice nucleation activity in the widespread soil fungus Mortierella alpina, Biogeosciences, 12, 1057-1071, 10.5194/bg-12-1057-2015, 2015.

Gallavardin, S. J., Froyd, K. D., Lohmann, U., Moehler, O., Murphy, D. M., and Cziczo, D. J.: Single Particle Laser Mass Spectrometry Applied to Differential Ice Nucleation Experiments at the AIDA Chamber, Aerosol Sci Tech, 42, 773-791, 2008.

Govindarajan, A. G., and Lindow, S. E.: Size of bacterial ice-nucleation sites measured in situ by radiation inactivation analysis, Proceedings of the National Academy of Sciences, 85, 1334-1338, 1988.

Hader, J. D., Wright, T. P., and Petters, M. D.: Contribution of pollen to atmospheric ice nuclei concentrations, Atmos. Chem. Phys., 14, 5433-5449, 10.5194/acp-14-5433-2014, 2014.

Hartmann, S., Augustin, S., Clauss, T., Wex, H., Šantl-Temkiv, T., Voigtländer, J., Niedermeier, D., and Stratmann, F.: Immersion freezing of ice nucleation active protein complexes, Atmos. Chem. Phys., 13, 5751-5766, 10.5194/acp-13-5751-2013, 2013.

Hiranuma, N., Mohler, O., Yamashita, K., Tajiri, T., Saito, A., Kiselev, A., Hoffmann, N., Hoose, C., Jantsch, E., Koop, T., and Murakami, M.: Ice nucleation by cellulose and its potential contribution to ice formation in clouds, Nat Geosci, 8, 273-277, 2015.

Hiranuma, N., Möhler, O., Kulkarni, G., Schnaiter, M., Vogt, S., Vochezer, P., Jarvinen, E., Wagner, R., Bell, D. M., Wilson, J., Zelenyuk, A., and Cziczo, D. J.: Development and characterization of an ice-selecting pumped counterflow virtual impactor (IS-PCVI) to study ice crystal residuals, Atmos Meas Tech, 9, 3817-3836, 10.5194/amt-9-3817-2016, 2016.

Hiranuma, N., and Möhler, O.: Personal Communication, 2018.

Hoose, C., Kristjansson, J. E., and Burrows, S. M.: How important is biological ice nucleation in clouds on a global scale?, Environ Res Lett, 5, 2010.

IPCC: Summary for Policymakers. In: Climate Change 2013: The Physical Science Basis. Contribution of Working Group I to the Fifth Assessment Report of the Intergovernmental Panel on Climate Change, Cambridge, United Kingdom and New York, NY, USA, 1–30, 2013.

Lindow, S. E., Arny, D. C., and Upper, C. D.: Bacterial Ice Nucleation - a Factor in Frost Injury to Plants, Plant Physiol, 70, 1084-1089, 1982.

Lindow, S. E., Lahue, E., Govindarajan, A. G., Panopoulos, N. J., and Gies, D.: Localization of Ice Nucleation Activity and the Icec Gene-Product in Pseudomonas-Syringae and Escherichia-Coli, Mol Plant Microbe In, 2, 262-272, Doi 10.1094/Mpmi-2-262, 1989.

Liu, P. S. K., Deng, R., Smith, K. A., Williams, L. R., Jayne, J. T., Canagaratna, M. R., Moore, K., Onasch, T. B., Worsnop, D. R., and Deshler, T.: Transmission efficiency of an aerodynamic focusing lens system: Comparison of model calculations and laboratory measurements for the Aerodyne Aerosol Mass Spectrometer, Aerosol Sci Tech, 41, 721-733, 2007.

Maki, L. R., Galyan, E. L., Changchi.Mm, and Caldwell, D. R.: Ice Nucleation Induced by Pseudomonas-Syringae, Appl Microbiol, 28, 456-459, 1974.

Maki, L. R., and Willoughby, K. J.: Bacteria as Biogenic Sources of Freezing Nuclei, J Appl Meteorol, 17, 1049-1053, Doi 10.1175/1520-0450(1978)017<1049:Babsof>2.0.Co;2, 1978.

Möhler, O., Stetzer, O., Schaefers, S., Linke, C., Schnaiter, M., Tiede, R., Saathoff, H., Kramer, M., Mangold, A., Budz, P., Zink, P., Schreiner, J., Mauersberger, K., Haag, W., Karcher, B., and Schurath, U.: Experimental investigation of homogeneous freezing of sulphuric acid particles in the aerosol chamber AIDA, Atmos Chem Phys, 3, 211-223, 2003.

Möhler, O., DeMott, P. J., Vali, G., and Levin, Z.: Microbiology and atmospheric processes: the role of biological particles in cloud physics, Biogeosciences, 4, 1059-1071, 2007.

Möhler, O., Georgakopoulos, D. G., Morris, C. E., Benz, S., Ebert, V., Hunsmann, S., Saathoff, H., Schnaiter, M., and Wagner, R.: Heterogeneous ice nucleation activity of bacteria: new laboratory experiments at simulated cloud conditions, Biogeosciences, 5, 1425-1435, 2008.

Morris, C. E., Georgakopoulos, D. G., and Sands, D. C.: Ice nucleation active bacteria and their potential role in precipitation, J Phys Iv, 121, 87-103, DOI 10.1051/jp4:2004121004, 2004.

Murray, B. J., O'Sullivan, D., Atkinson, J. D., and Webb, M. E.: Ice nucleation by particles immersed in supercooled cloud droplets, Chem Soc Rev, 41, 6519-6554, 10.1039/c2cs35200a, 2012.

O'Sullivan, D., Murray, B. J., Ross, J. F., and Webb, M. E.: The adsorption of fungal ice-nucleating proteins on mineral dusts: a terrestrial reservoir of atmospheric ice-nucleating particles, Atmos. Chem. Phys., 16, 7879-7887, 10.5194/acp-16-7879-2016, 2016.

Oehm, C. C., C.; Amato, P.; Attard, E.; Delort, A.-M.; Morris, C.; Kiselev, A.; Stetzer, O.; Möhler, O.; Leisner, T.: Laboratory studies with cloud-derived Bacterial Cells acting as Ice Nuclei in the Immersion and Deposition Mode, EGU General Assembly 2012, Vienna, Austria, 2012, 399,

Pandey, R., Usui, K., Livingstone, R. A., Fischer, S. A., Pfaendtner, J., Backus, E. H. G., Nagata, Y., Frohlich-Nowoisky, J., Schmuser, L., Mauri, S., Scheel, J. F., Knopf, D. A., Poschl, U., Bonn, M., and Weidner, T.: Ice-nucleating bacteria control the order and dynamics of interfacial water, Sci Adv, 2, 2016.

Peters, T. M., Ott, D., and O'Shaughnessy, P. T.: Comparison of the Grimm 1.108 and 1.109 portable aerosol spectrometer to the TSI 3321 aerodynamic particle sizer for dry particles, Ann Occup Hyg, 50, 843-850, 2006.

Phillips, V. T. J., Andronache, C., Christner, B., Morris, C. E., Sands, D. C., Bansemer, A., Lauer, A., McNaughton, C., and Seman, C.: Potential impacts from biological aerosols on ensembles of continental clouds simulated numerically, Biogeosciences, 6, 987-1014, 2009.

Polen, M., Lawlis, E., and Sullivan, R. C.: The unstable ice nucleation properties of Snomax (R) bacterial particles, J Geophys Res-Atmos, 121, 11666-11678, 2016.

Pratt, K. A., DeMott, P. J., French, J. R., Wang, Z., Westphal, D. L., Heymsfield, A. J., Twohy, C. H., Prenni, A. J., and Prather, K. A.: In situ detection of biological particles in cloud ice-crystals, Nature Geosci, 2, 398-401 (SI section), http://www.nature.com/ngeo/journal/v2/n6/suppinfo/ngeo521_S1.html, 2009.

Pruppacher, H. R., and Klett, J. D.: Microphysics of Clouds and Precipitation, Atmospheric and Oceanographic Sciences Library, Springer Netherlands, 2010.

Pummer, B. G., Bauer, H., Bernardi, J., Bleicher, S., and Grothe, H.: Suspendable macromolecules are responsible for ice nucleation activity of birch and conifer pollen, Atmos. Chem. Phys., 12, 2541-2550, 10.5194/acp-12-2541-2012, 2012.

Šantl-Temkiv, T., Sahyoun, M., Finster, K., Hartmann, S., Augustin-Bauditz, S., Stratmann, F., Wex, H., Clauss, T., Nielsen, N. W., Sørensen, J. H., Korsholm, U. S., Wick, L. Y., and Karlson, U. G.: Characterization of airborne ice-nucleation-active bacteria and bacterial fragments, Atmospheric Environment, 109, 105-117, http://dx.doi.org/10.1016/j.atmosenv.2015.02.060, 2015.

Schnell, R. C., and Vali, G.: Biogenic Ice Nuclei: Part I. Terrestrial and Marine Sources, Journal of the Atmospheric Sciences, 33, 1554-1564, 10.1175/1520-0469(1976)033<1554:BINPIT>2.0.CO;2, 1976.

Sharma, P. K., and Rao, K. H.: Analysis of different approaches for evaluation of surface energy of microbial cells by contact angle goniometry, Adv Colloid Interfac, 98, 341-463, Pii S0001-8686(02)00004-0

Doi 10.1016/S0001-8686(02)00004-0, 2002.

Simpson, E. L., Connolly, P. J., and McFiggans, G. B.: Competition for water vapour results in suppression of ice formation in mixed phase clouds, Atmos. Chem. Phys. Discuss., 10.5194/acp-2017-673, 2017.

Spracklen, D. V., and Heald, C. L.: The contribution of fungal spores and bacteria to regional and global aerosol number and ice nucleation immersion freezing rates, Atmos. Chem. Phys., 14, 9051-9059, 10.5194/acp-14-9051-2014, 2014.

Srivastava, A., Pitesky, M. E., Steele, P. T., Tobias, H. J., Fergenson, D. P., Horn, J. M., Russell, S. C., Czerwieniec, G. A., Lebrilla, C. S., Gard, E. E., and Frank, M.: Comprehensive assignment of mass spectral signatures from individual Bacillus atrophaeus spores in matrix-free laser desorption/ionization bioaerosol mass spectrometry, Anal Chem, 77, 3315-3323, 2005.

Turner, M. A., Arellano, F., and Kozloff, L. M.: 3 Separate Classes of Bacterial Ice Nucleation Structures, J Bacteriol, 172, 2521-2526, 1990.

Turner, M. A., Arellano, F., and Kozloff, L. M.: Components of Ice Nucleation Structures of Bacteria, J Bacteriol, 173, 6515-6527, 1991.

Vaden, T. D., Imre, D., Beranek, J., and Zelenyuk, A.: Extending the Capabilities of Single Particle Mass Spectrometry: I. Measurements of Aerosol Number Concentration, Size Distribution, and Asphericity, Aerosol Sci Tech, 45, 113-124, 10.1080/02786826.2010.526155, 2011a.

Vaden, T. D., Imre, D., Beranek, J., and Zelenyuk, A.: Extending the Capabilities of Single Particle Mass Spectrometry: II. Measurements of Aerosol Particle Density without DMA, Aerosol Sci Tech, 45, 125-135, Doi 10.1080/02786826.2010.526156, 2011b.

Vali, G., Christensen, M., Fresh, R. W., Galyan, E. L., Maki, L. R., and Schnell, R. C.: Biogenic Ice Nuclei .2. Bacterial Sources, Journal of the Atmospheric Sciences, 33, 1565-1570, 1976.

Vali, G., Rogers, D. C., Gordon, D., Saunders,, C. P. R., R., M.,, and Black, R.: Aerosol and Nucleation Research. In Support of NASA Cloud Physics Experiments in Space, NASA Final Report, 1–86, 1978.

Vali, G., DeMott, P. J., Möhler, O., and Whale, T. F.: Technical Note: A proposal for ice nucleation terminology, Atmos Chem Phys, 15, 10263-10270, 2015.

Wagner, R., and Möhler, O.: Heterogeneous ice nucleation ability of crystalline sodium chloride dihydrate particles, J Geophys Res-Atmos, 118, 4610-4622, 2013.

Wex, H., Augustin-Bauditz, S., Boose, Y., Budke, C., Curtius, J., Diehl, K., Dreyer, A., Frank, F., Hartmann, S., Hiranuma, N., Jantsch, E., Kanji, Z. A., Kiselev, A., Koop, T., Möhler, O., Niedermeier, D., Nillius, B., Rosch, M., Rose, D., Schmidt, C., Steinke, I., and Stratmann, F.: Intercomparing different devices for the investigation of ice nucleating particles using Snomax (R) as test substance, Atmos Chem Phys, 15, 1463-1485, 10.5194/acp-15-1463-2015, 2015.

Wilson, J., Imre, D., Beranek, J., Shrivastava, M., and Zelenyuk, A.: Evaporation Kinetics of Laboratory-Generated Secondary Organic Aerosols at Elevated Relative Humidity, Environ Sci Technol, 49, 243-249, 10.1021/es505331d, 2015.

Wolber, P. K., Deininger, C. A., Southworth, M. W., Vandekerckhove, J., Vanmontagu, M., and Warren, G. J.: Identification and Purification of a Bacterial Ice-Nucleation Protein, P Natl Acad Sci USA, 83, 7256-7260, DOI 10.1073/pnas.83.19.7256, 1986.

Wolf, R., Slowik, J. G., Schaupp, C., Amato, P., Saathoff, H., Möhler, O., Prevot, A. S. H., and Baltensperger, U.: Characterization of ice-nucleating bacteria using on-line electron impact ionization aerosol mass spectrometry, J Mass Spectrom, 50, 662-671, 10.1002/jms.3573, 2015.

Yankofsky, S. A., Levin, Z., Bertold, T., and Sandlerman, N.: Some Basic Characteristics of Bacterial Freezing Nuclei, J Appl Meteorol, 20, 1013-1019, Doi 10.1175/1520-0450(1981)020<1013:Sbcobf>2.0.Co;2, 1981.

Zawadowicz, M. A., Froyd, K. D., Murphy, D. M., and Cziczo, D. J.: Improved identification of primary biological aerosol particles using single-particle mass spectrometry, Atmos. Chem. Phys., 17, 7193-7212, 10.5194/acp-17-7193-2017, 2017.

Zelenyuk, A., Cuadra-Rodriguez, L. A., Imre, D., Shimpi, S., and Warey, A.: Comprehensive Characterization Of Ultrafine Particulate Emission From 2007 Diesel Engines: PM Size Distribution, Loading And Individual Particle Size And Composition, *Eos Trans. AGU*, 2006, Abstract A43A-0121,

Zelenyuk, A., Imre, D., Nam, E. J., Han, Y. P., and Mueller, K.: ClusterSculptor: Software for expert-steered classification of single particle mass spectra, Int J Mass Spectrom, 275, 1-10, 10.1016/j.ijms.2008.04.033, 2008.

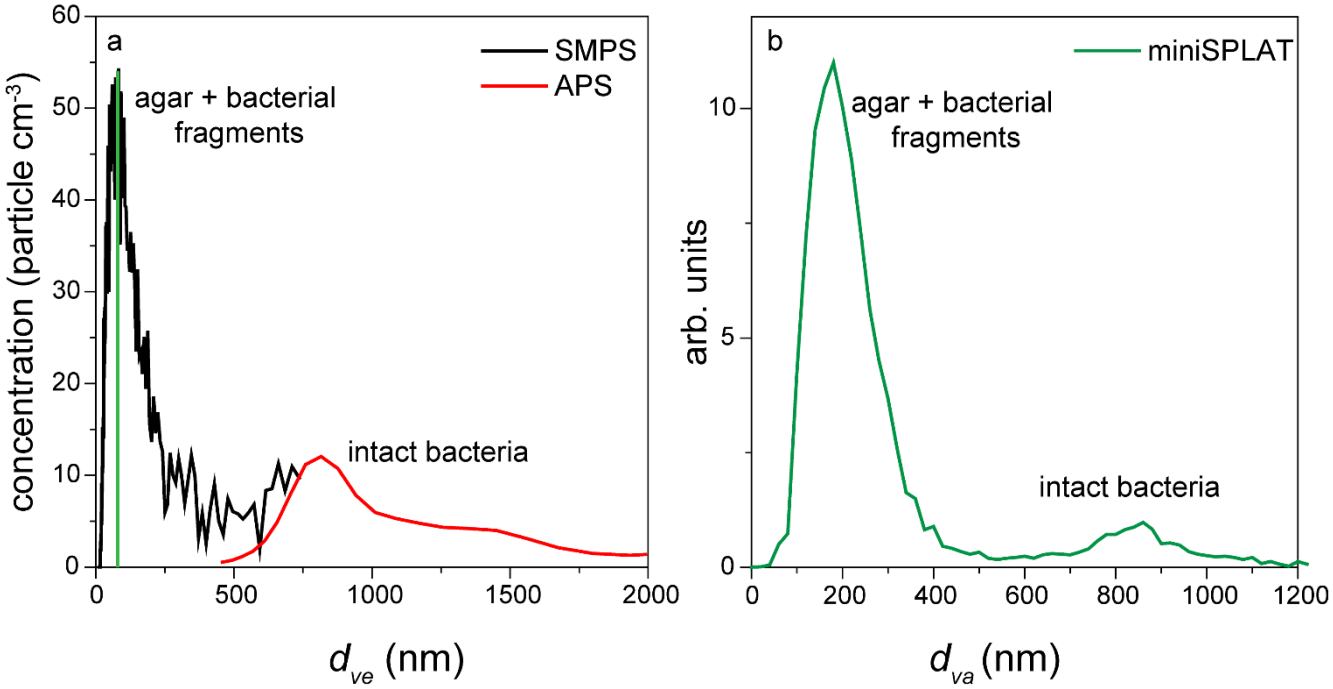

Figure 1: Size distributions of an aerosolized suspension of Pseudomonas syringae in the AIDA cloud chamber before Expansion 1, calculated based on the SMPS and the APS measurements (a) and miniSPLAT (b). The miniSPLAT small particle detection limit is denoted by the green line in (a).

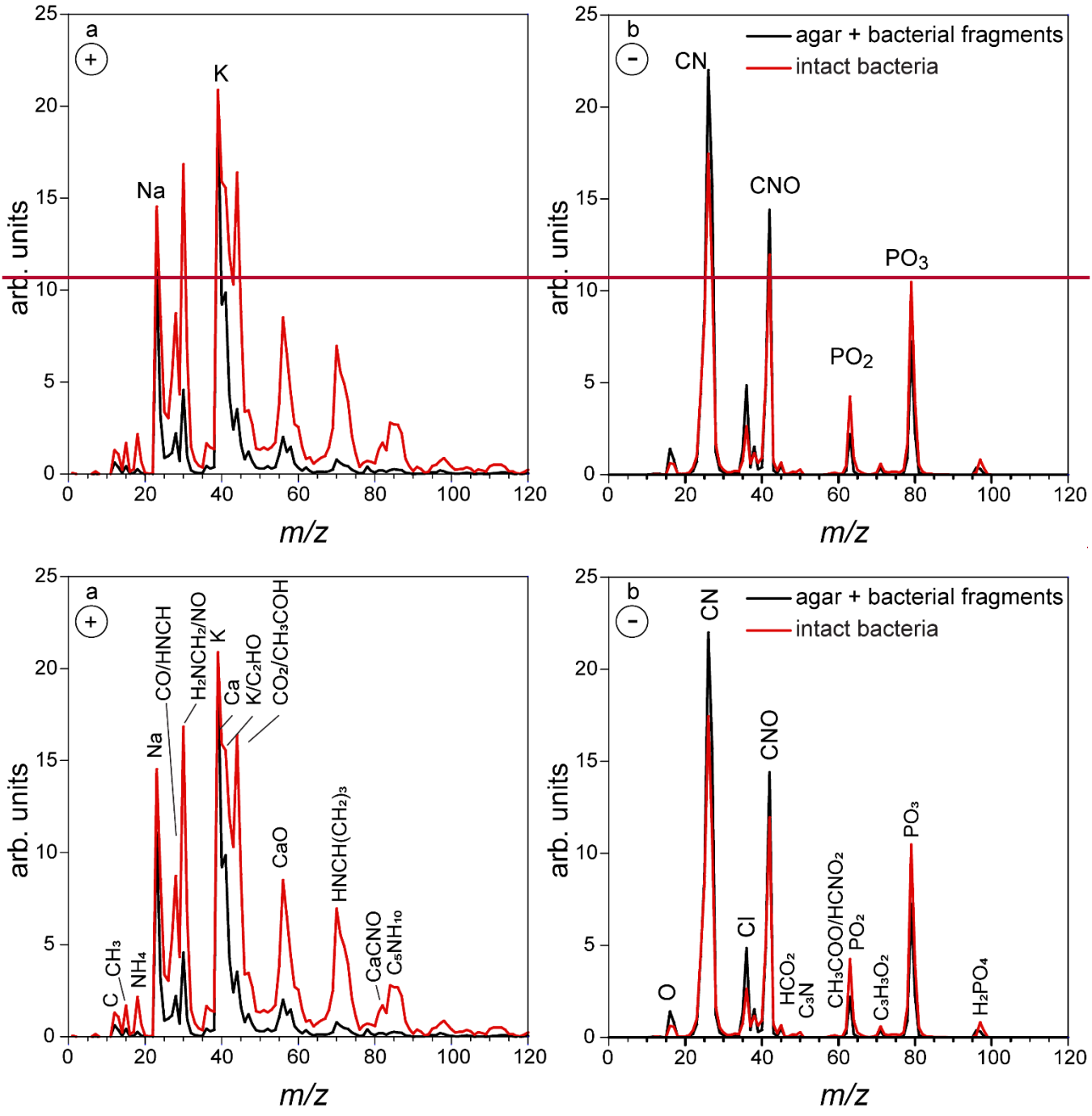
a
b
agar + bacterial fragments
intact bacteria
arb. units
m/z
Na
K
CN
CNO
PO2
PO3
C
CH3
NH4
CO/HNCH
H2NCH2/NO
Ca
K/C2HO
CO2/CH3COH
CaO
HNCH(CH2)3
CaCNO
C5NH10
O
Cl
HCO2
C3N
CH3COO/HCNO2
C3H3O2
H2PO4

Figure 2: Positive (a) and negative (b) average mass spectra of the particles in the AIDA chamber, measured before Expansion 1. Reference mass spectra of the small size mode, made up of ~~agar mixed with~~ bacterial fragments mixed with agar, which includes particles smaller than 300 nm, are marked in black, and the mass spectra of the large size mode particles (d_{va} > 700 nm), composed of intact Pseudomonas syringae bacterial cells, are marked in red.

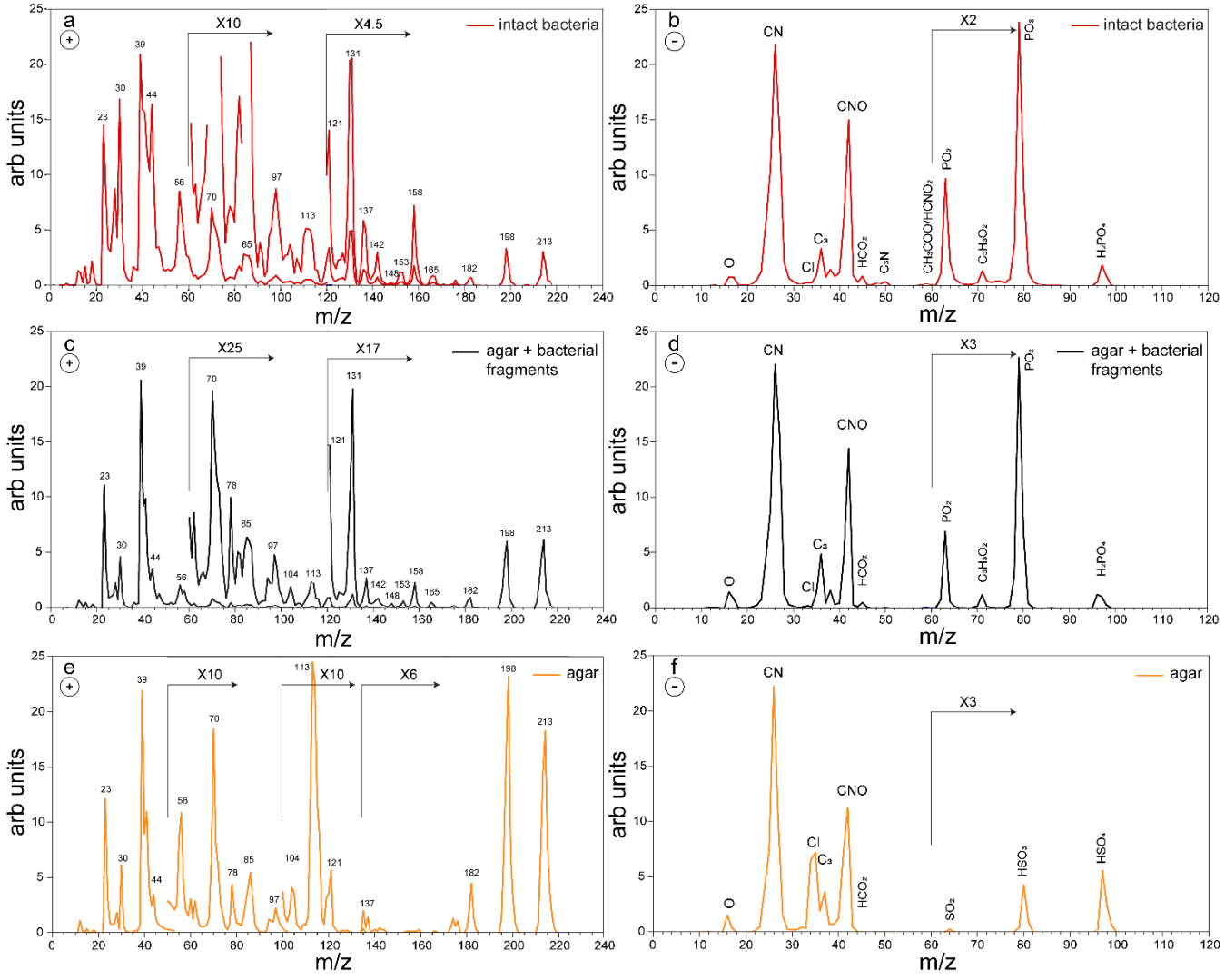

Figure 3: Positive (a) and negative (b) MS of intact Pseudomonas syringae bacteria measured before Expansion 1; Positive (c) and negative (d) MS of the small particles mode, measured before Expansion 1; Positive (e) and negative (f) MS of pure agar particles measured in a separate experiment.

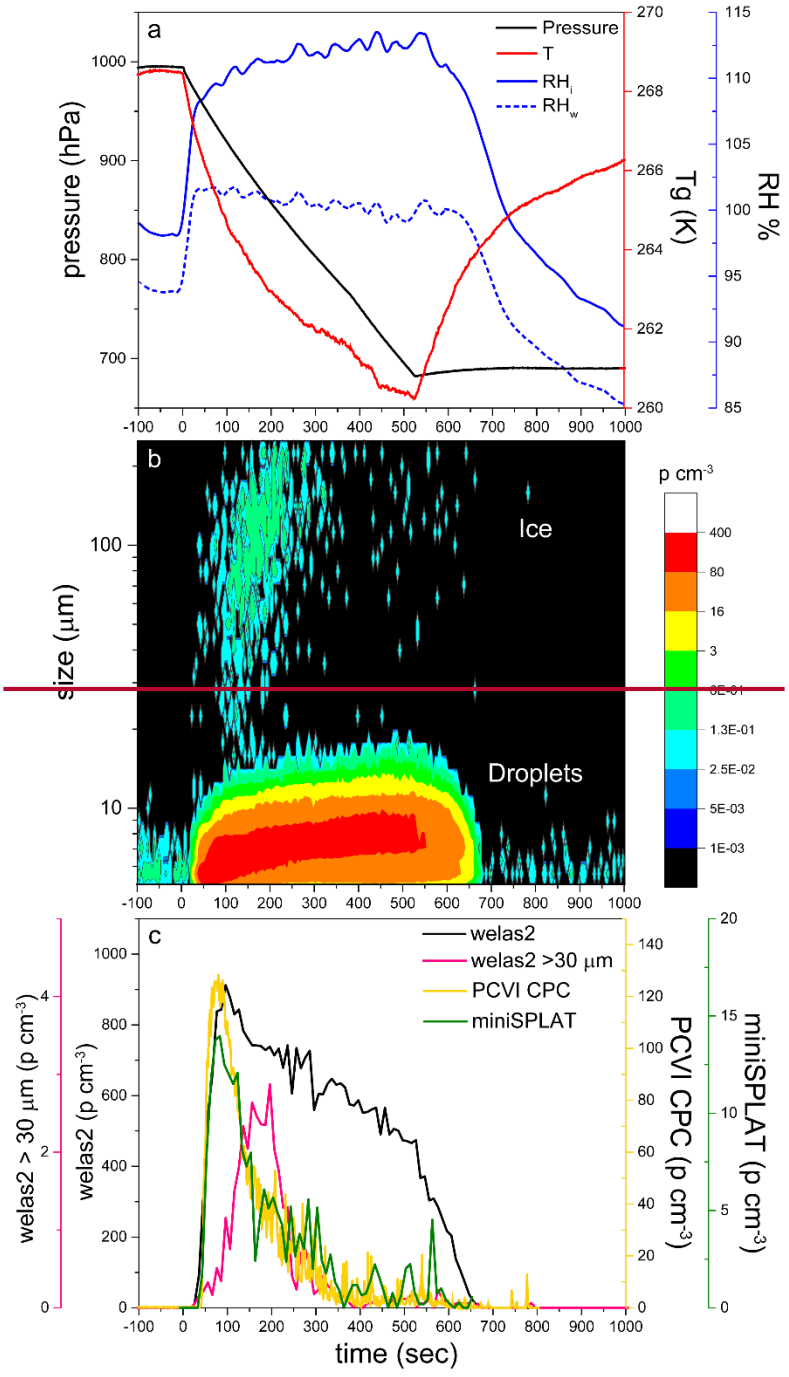
a
Pressure
T
RH$_i$
RH$_w$
pressure (hPa)
Tg (K)
RH %
b
Ice
Droplets
size (µm)
p cm^{-3}
400
80
16
3
1.3E-01
2.5E-02
5E-03
1E-03
c
welas2
welas2 >30 µm
PCVI CPC
miniSPLAT
welas2 > 30 µm (p cm^{-3})
welas2 (p cm^{-3})
PCVI CPC (p cm^{-3})
miniSPLAT (p cm^{-3})
time (sec)

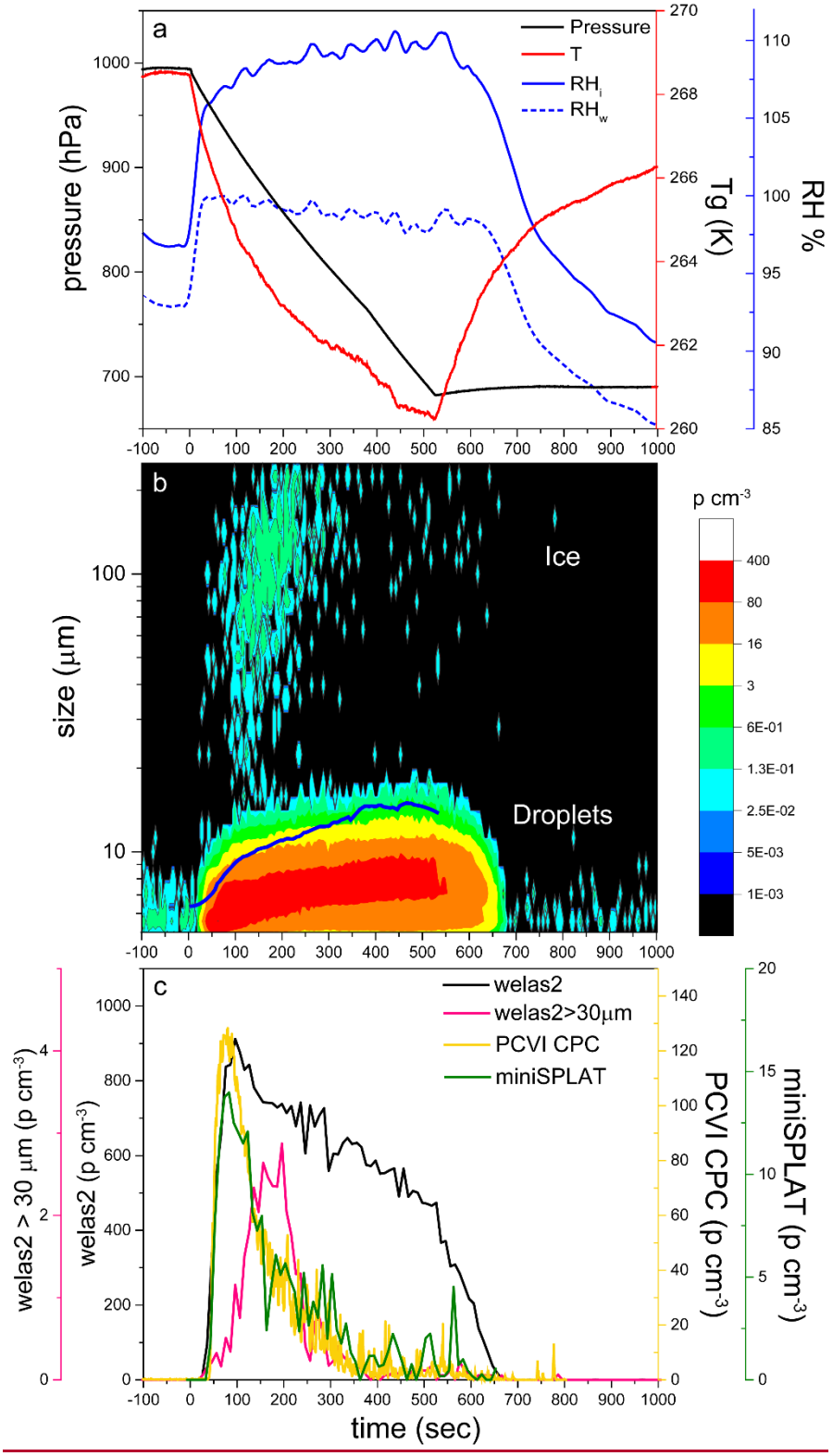
a
Pressure
T
RH$_i$
RH$_w$
pressure (hPa)
Tg (K)
RH %
b
Ice
Droplets
size (µm)
p cm^{-3}
400
80
16
3
6E-01
1.3E-01
2.5E-02
5E-03
1E-03
c
welas2
welas2>30µm
PCVI CPC
miniSPLAT
welas2 > 30 µm (p cm^{-3})
welas2 (p cm^{-3})
PCVI CPC (p cm^{-3})
miniSPLAT (p cm^{-3})
time (sec)

Figure 43: Data from Expansion 1 with Pseudomonas syringae bacteria. (a) The pressure (black) and the temperature of the gas (red) inside the AIDA chamber. The measured RH with respect to ice (RHi) and water (RHw) are indicated in solid and dashed blue lines, respectively; (b) the size distributions of the particles measured with welas2 during the expansion. Particles smaller than ~15 µm are liquid droplets, while particles with larger optical diameters are ice. The PCVI cut-size is shown by the blue trace; (c) The welas2-measured total particle number concentrations (black) and the number concentrations of particles larger than 30 µm (pink). The number concentrations of particles transmitted by the PCVI and measured by CPC and miniSPLAT are marked in yellow and green, respectively.

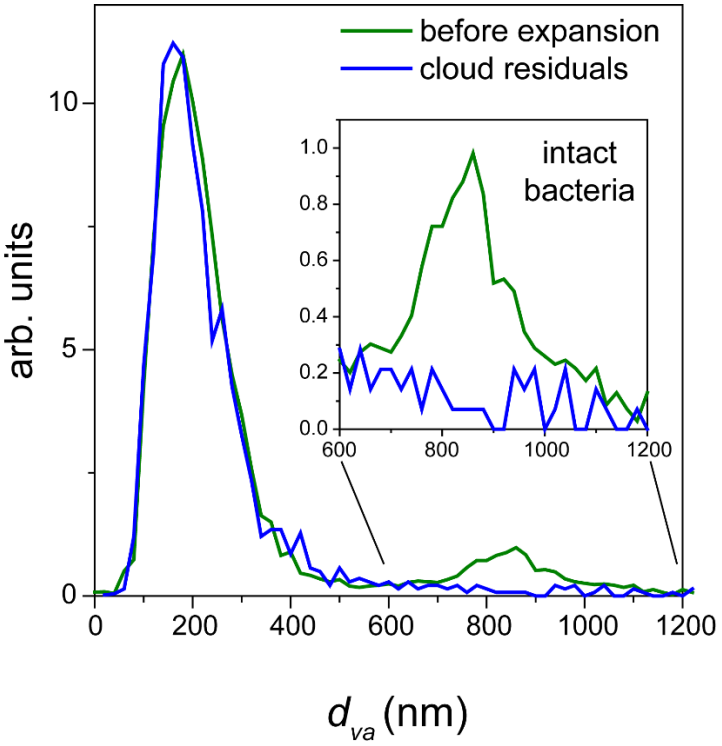

Figure 54: Normalized miniSPLAT-measured d_{va} size distributions of Pseudomonas syringae particles in the AIDA chamber before Expansion 1 (green) and of cloud residuals transmitted through the PCVI during the expansion (blue). The inset presents in expanded scale the size distributions of the intact bacteria, showing that cloud residuals do not exhibit the distinct peak for intact bacteria.

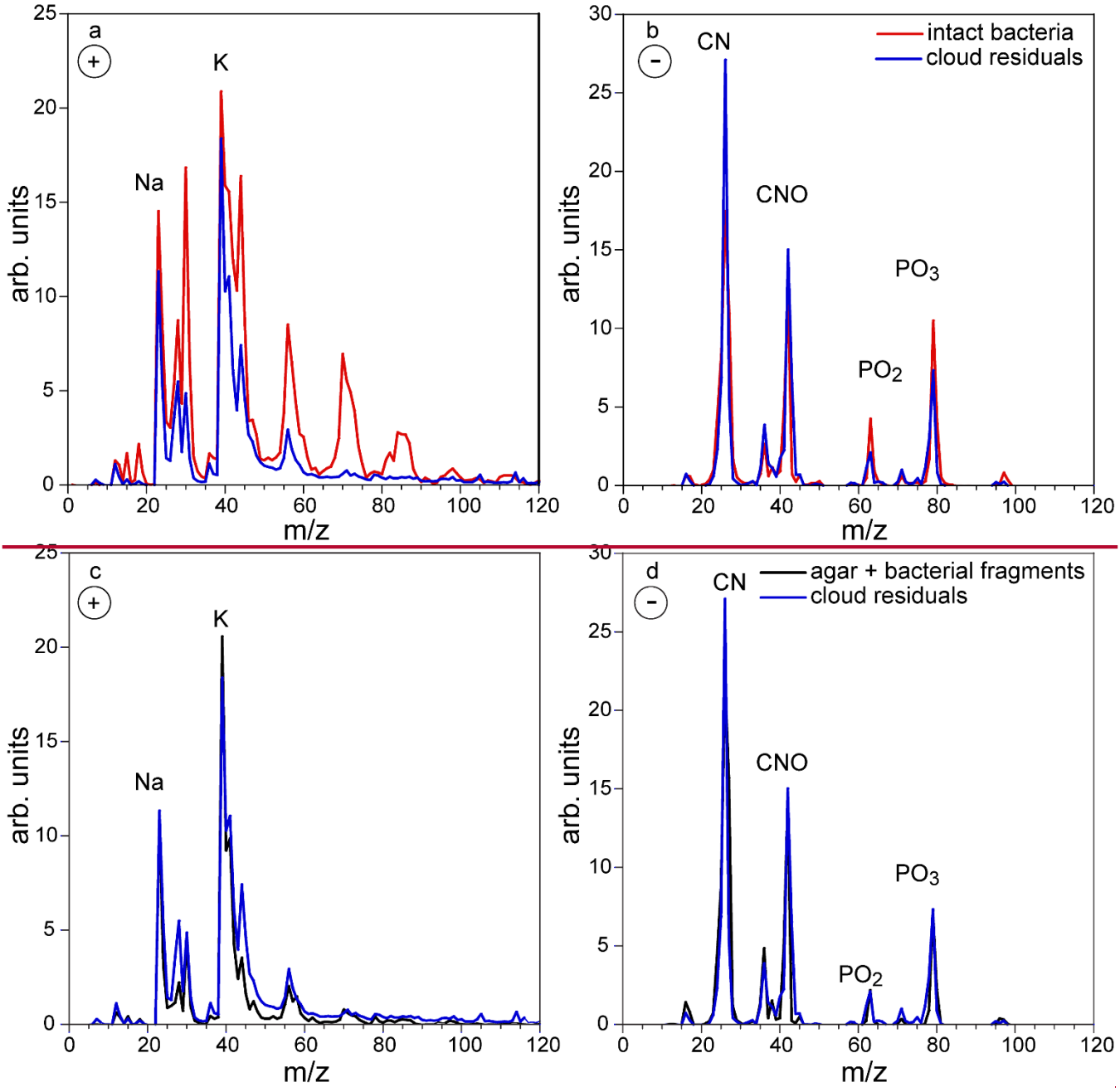
a
+
K
Na
arb. units
m/z
b
-
CN
CNO
PO3
PO2
intact bacteria
cloud residuals
arb. units
m/z
c
+
K
Na
arb. units
m/z
d
-
CN
CNO
PO3
PO2
agar + bacterial fragments
cloud residuals
arb. units
m/z

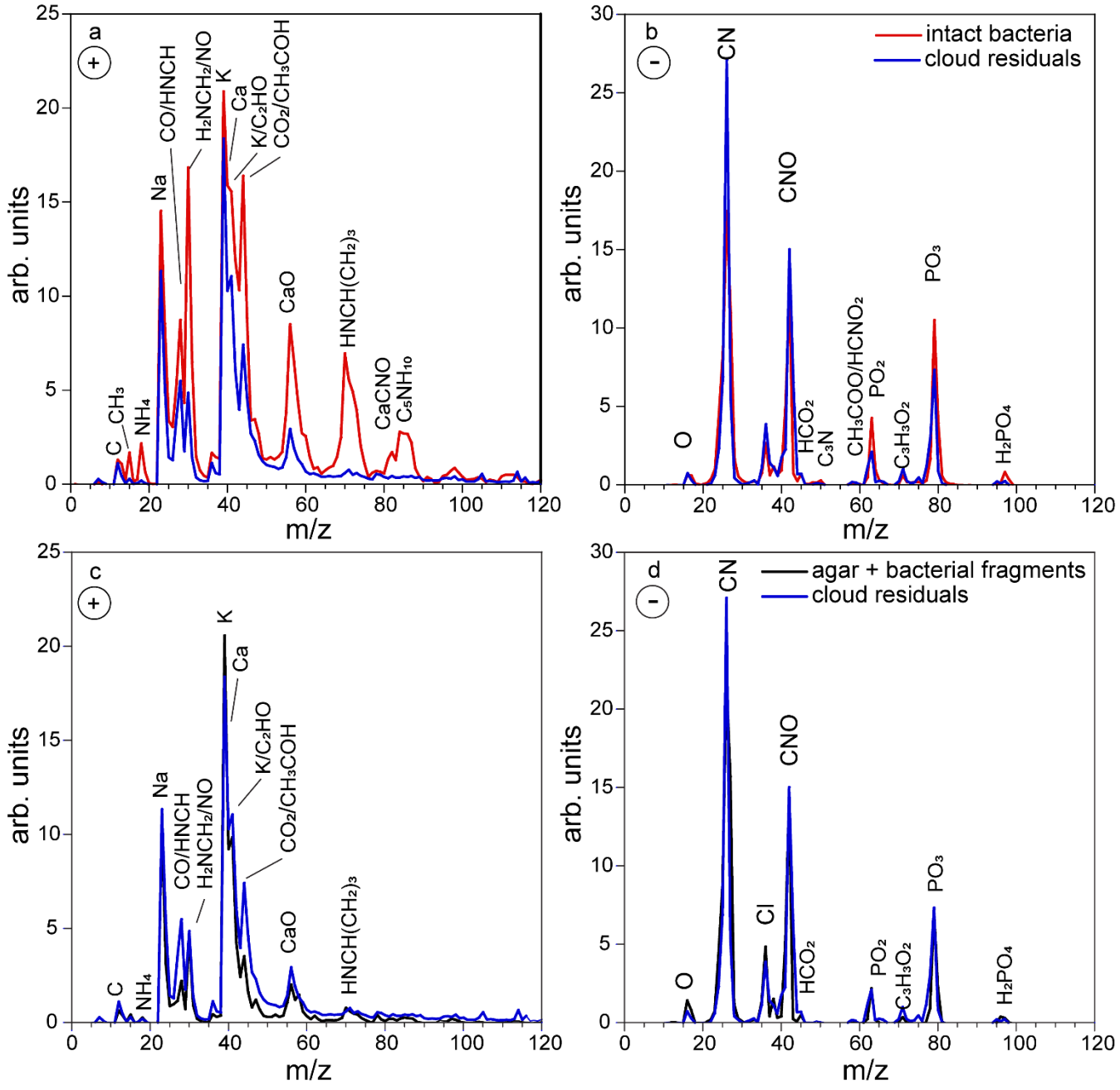

Figure ~~65~~: Positive (a) and negative (b) ion average mass spectra of cloud residuals sampled during Expansion 1 (blue) superimposed on the average MS of intact bacteria (red); (c) and (d) The same cloud residuals average MS superimposed on the reference average MS of the small particle mode, composed of Pseudomonas syringae bacterial fragments mixed with agar (black).

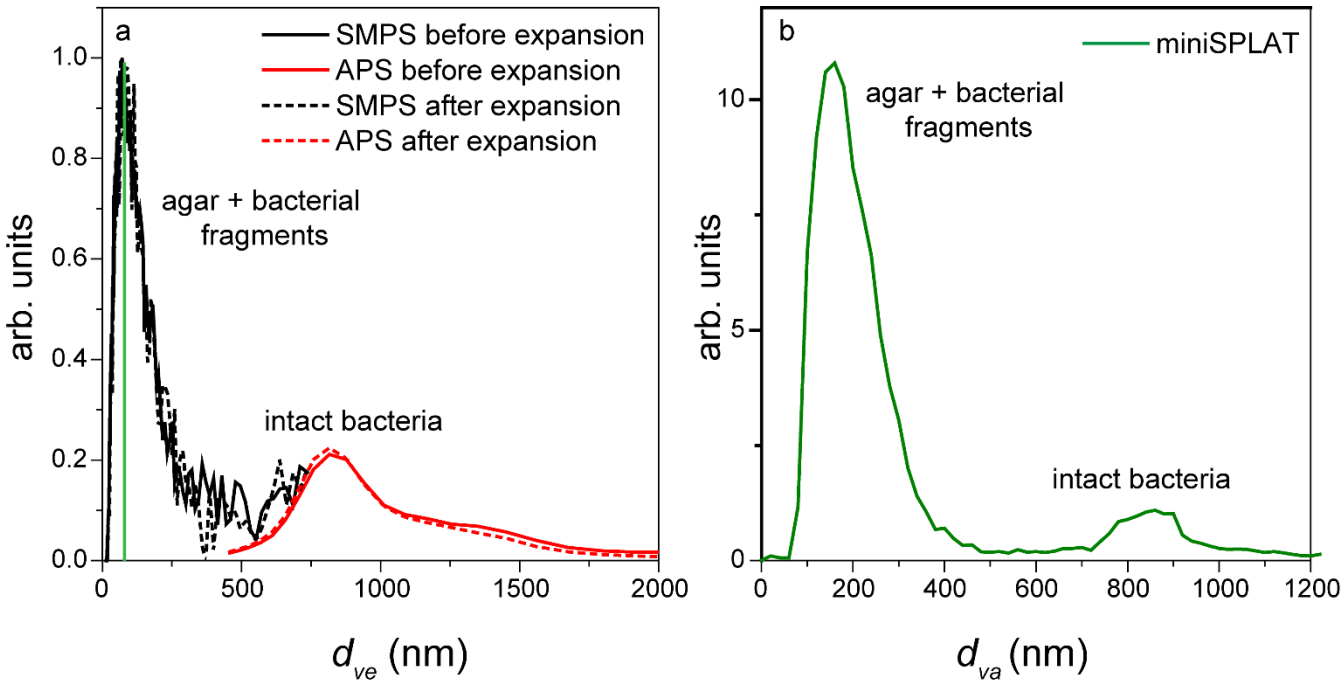

Figure 7~~6~~: (a) Size distributions of an aerosolized suspension of PF CGina particles in the AIDA cloud chamber before and after Expansion 2 calculated from the SMPS and the APS measurements; (b) miniSPLAT-measured size distribution of PF CGina particles in the chamber before Expansion 2. The miniSPLAT small particle detection limit is denoted by the green line in (a).

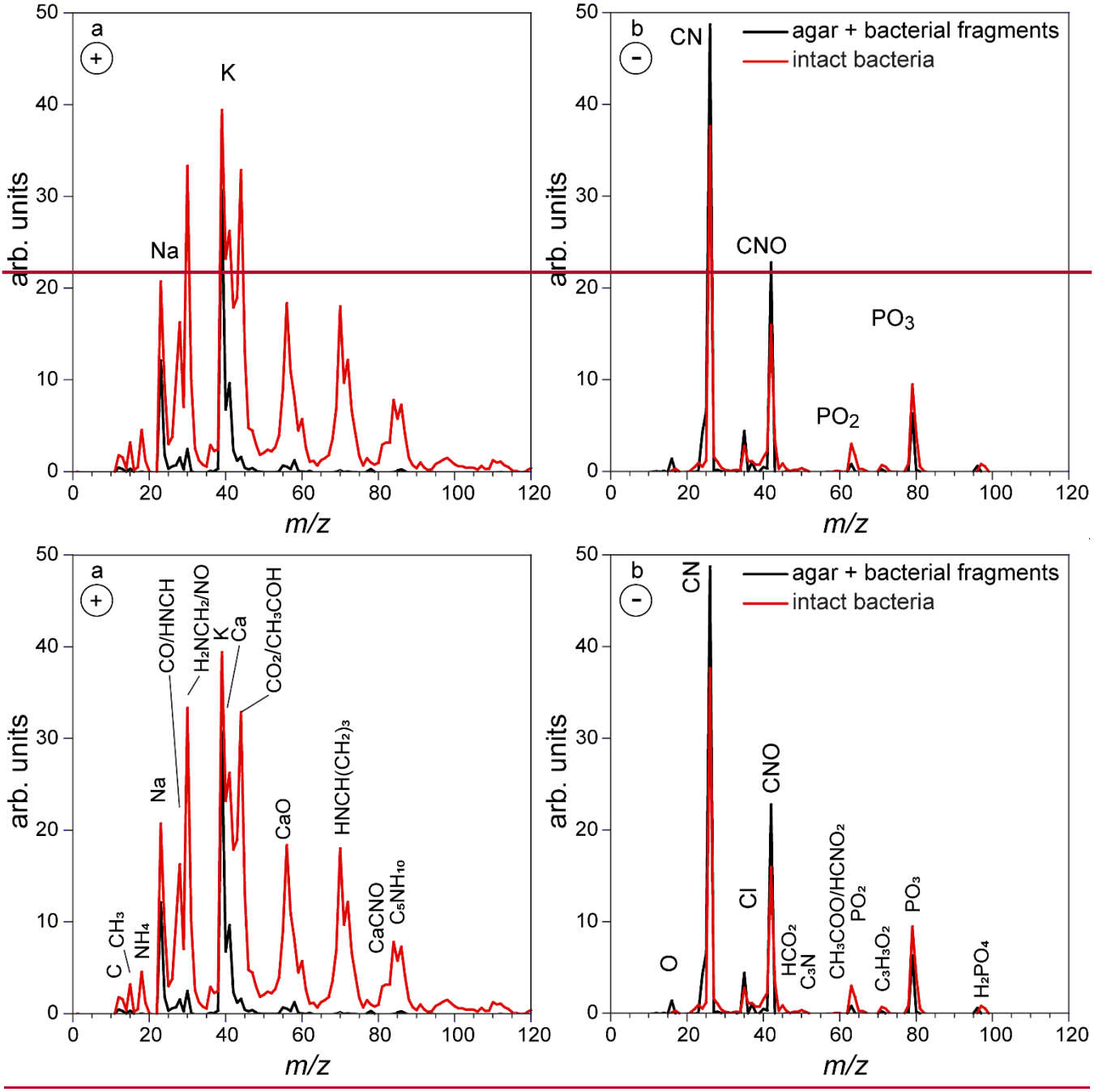

Figure 8~~7~~: Positive (a) and negative (b) average mass spectra of the particles in the AIDA chamber, measured before Expansion 2. Reference mass spectra of the small size mode, made up of particles smaller than 300 nm (black), and the mass spectra of the large size mode (>700 nm) composed of intact PF CGina bacterial cells are marked in red.

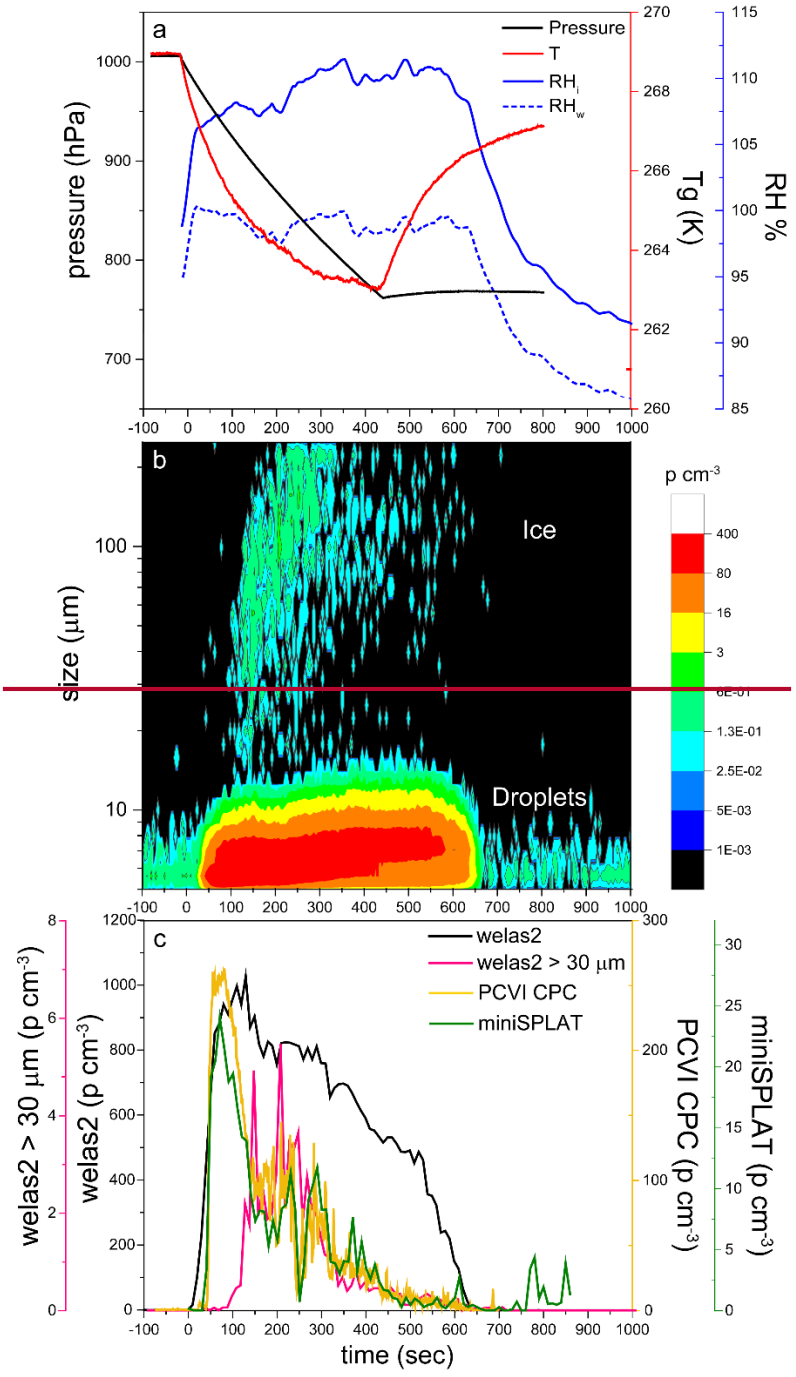
a
Pressure
T
RH$_i$
RH$_w$
pressure (hPa)
Tg (K)
RH %
b
Ice
Droplets
size (μm)
p cm^{-3}
400
80
16
3
1.3E-01
2.5E-02
5E-03
1E-03
c
welas2
welas2 > 30 μm
PCVI CPC
miniSPLAT
welas2 > 30 μm (p cm^{-3})
welas2 (p cm^{-3})
PCVI CPC (p cm^{-3})
miniSPLAT (p cm^{-3})
time (sec)

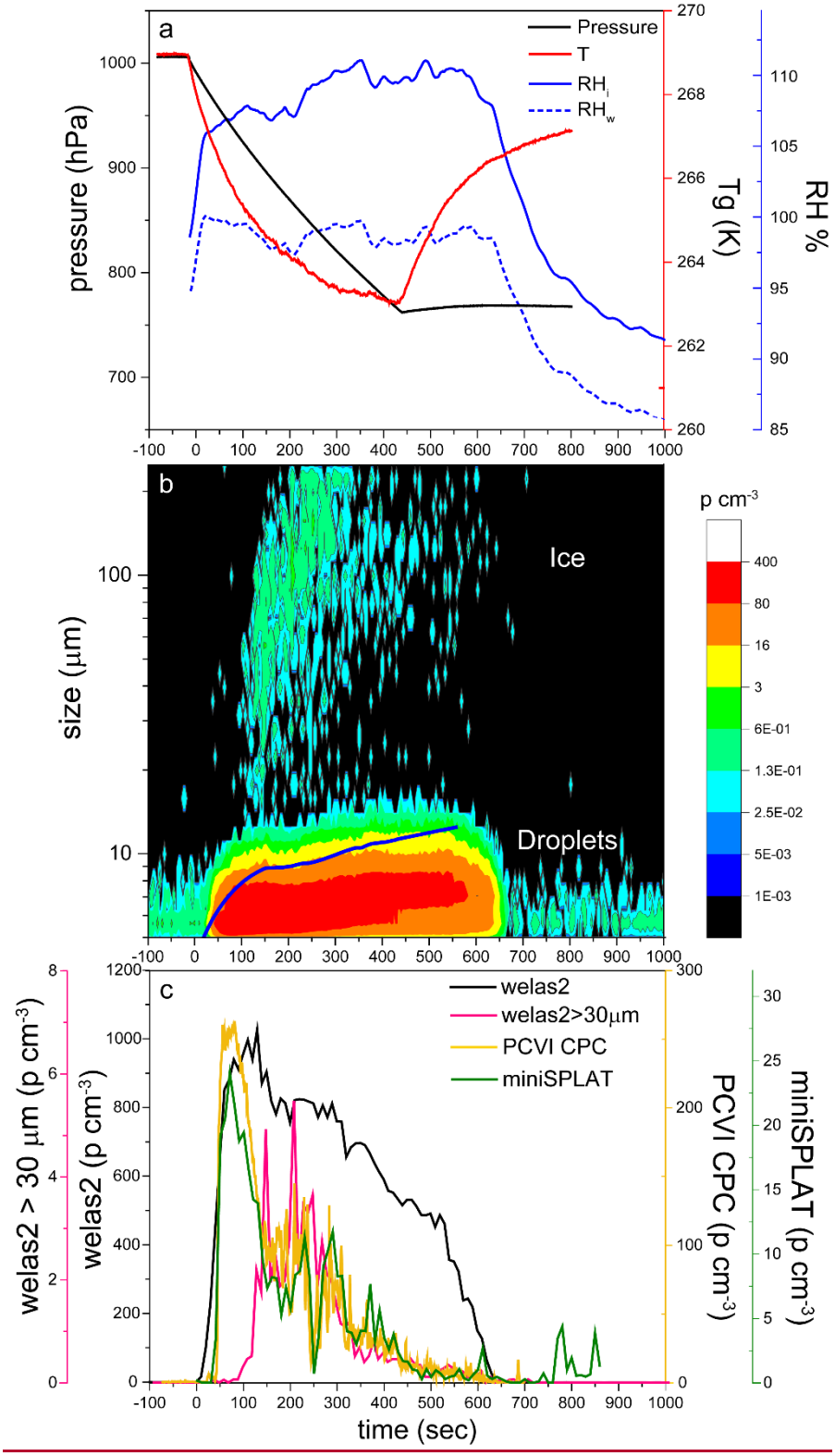
a
Pressure
T
RH$_i$
RH$_w$
pressure (hPa)
Tg (K)
RH %
b
Ice
Droplets
size (μm)
p cm^{-3}
400
80
16
3
6E-01
1.3E-01
2.5E-02
5E-03
1E-03
c
welas2
welas2>30μm
PCVI CPC
miniSPLAT
welas2 > 30 μm (p cm^{-3})
welas2 (p cm^{-3})
PCVI CPC (p cm^{-3})
miniSPLAT (p cm^{-3})
time (sec)

Figure 98: Data from Expansion 2 with PF CGina bacteria. (a) The pressure (black) and the temperature of the gas (red) inside the AIDA chamber. The measured RH with respect to ice (RHi) and water (RHw) are indicated in solid and dashed blue lines, respectively; (b) the size distributions of the particles measured with welas2 during the expansion. Particles smaller than ~15 µm are liquid droplets, while larger particles are ice. The PCVI cut-size is shown by the blue trace; (c) The welas2-measured total particle number concentrations (black) and the number concentrations of particles larger than 30 µm (pink). The number concentrations of particles transmitted by the PCVI and measured by CPC and miniSPLAT are marked in yellow and green, respectively.

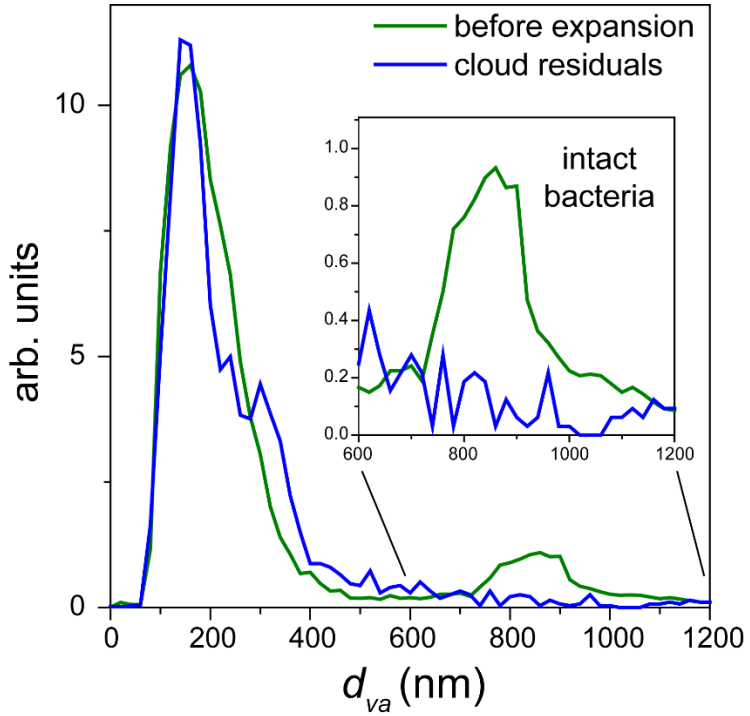

Figure 109: Normalized miniSPLAT-measured d_{va} size distributions of PF CGina particles in the AIDA chamber before Expansion 2 (green) and of cloud residuals transmitted through the PCVI during the expansion (blue). The inset presents in expanded scale the size distributions of the intact bacteria, showing that nearly no distinct peak for intact bacteria.

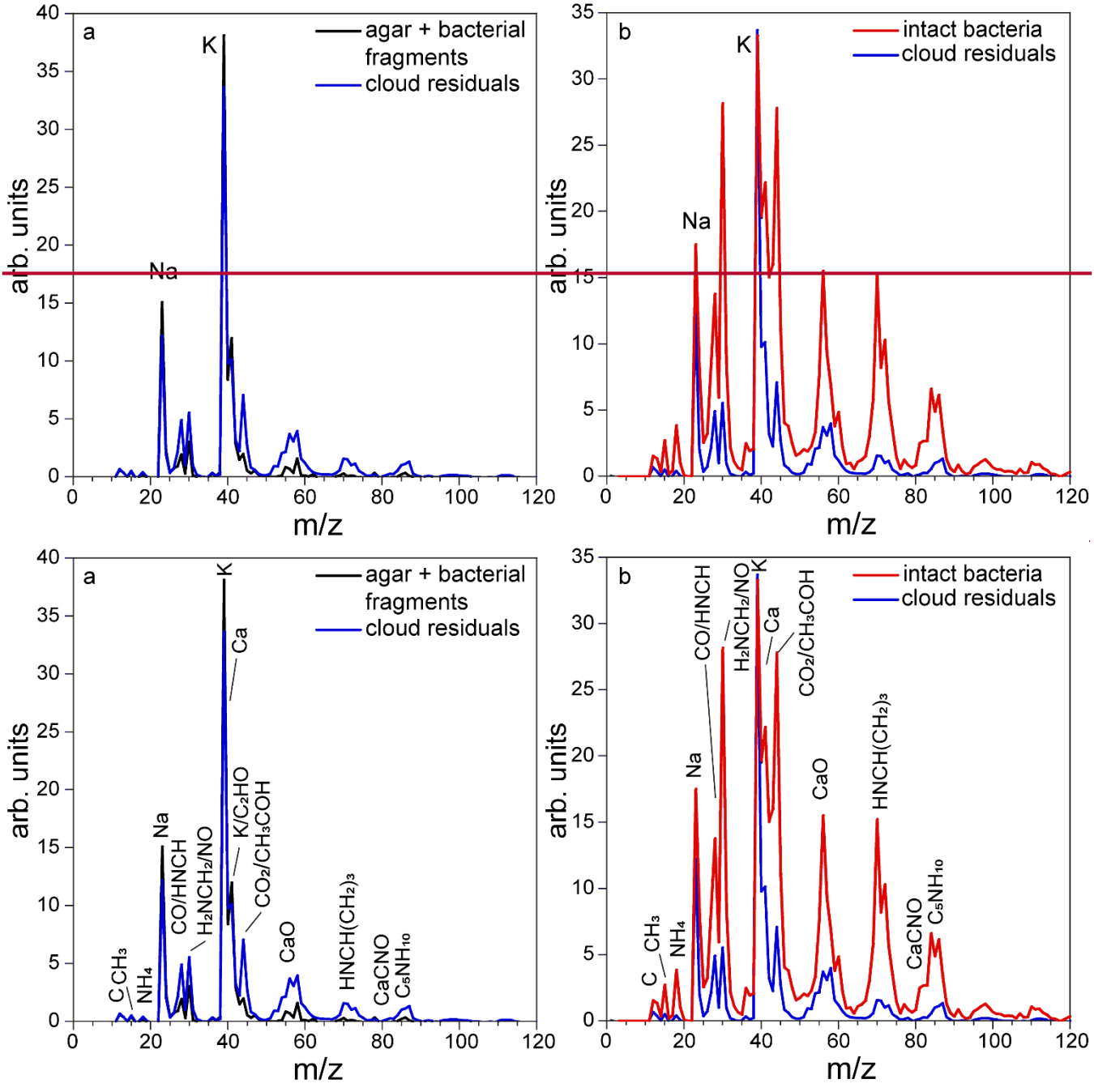

Figure 1~~0~~1: (a) Average r~~R~~eference MS of the small particle mode, composed of agar and PF CGina bacterial fragments, (black) and the average MS of cloud residuals acquired during Expansion 2 (blue); (b) average MS of intact bacteria (red) and the average MS of cloud residuals acquired during Expansion 2 (blue).

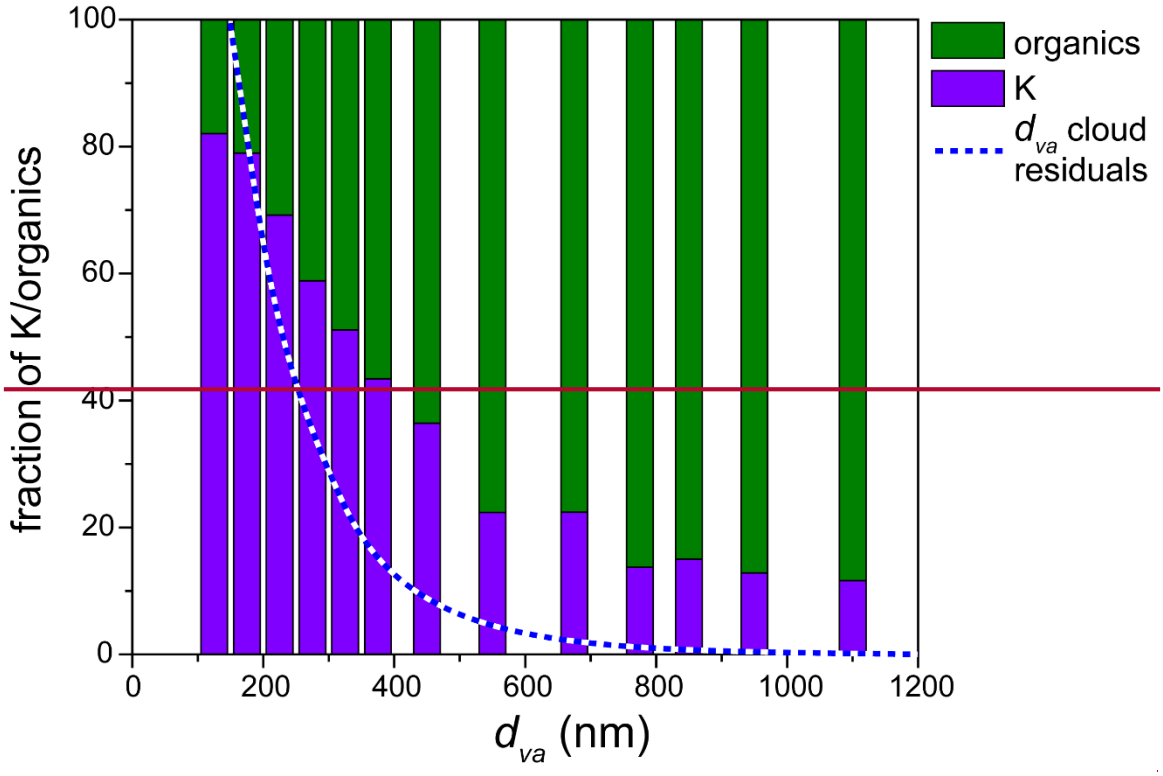
100
80
60
40
20
0
fraction of K/organics
0
200
400
600
800
1000
1200
d_{va} (nm)
organics
K
d_{va} cloud residuals

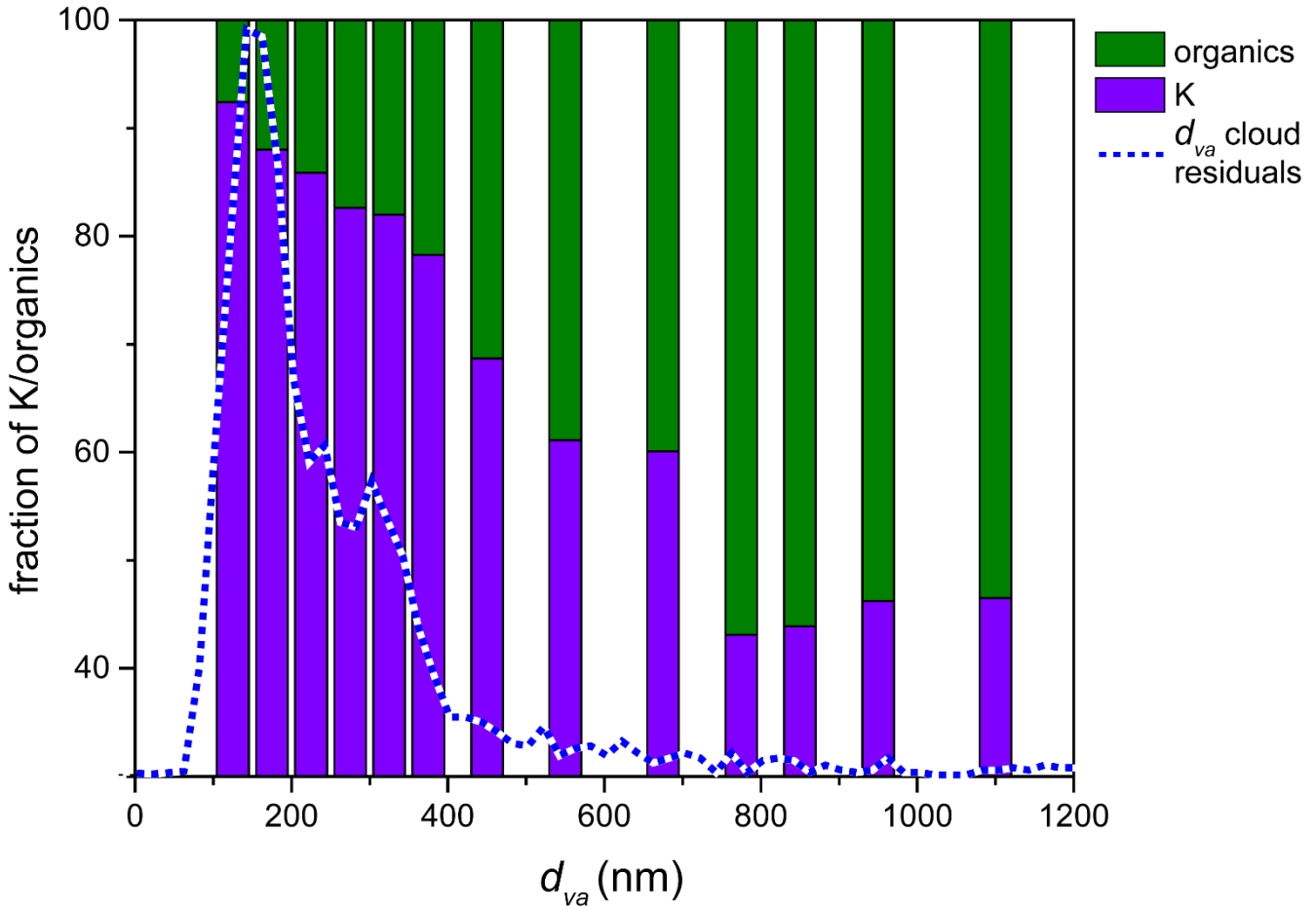

Figure 1~~2~~1: The relative mass spectral intensity of peaks assigned to organics and potassium as a function of particle d_{va}, showing that larger particles contain more organics for PF CGina bacteria. The dashed line represents the measured d_{va} distribution of cloud residuals.

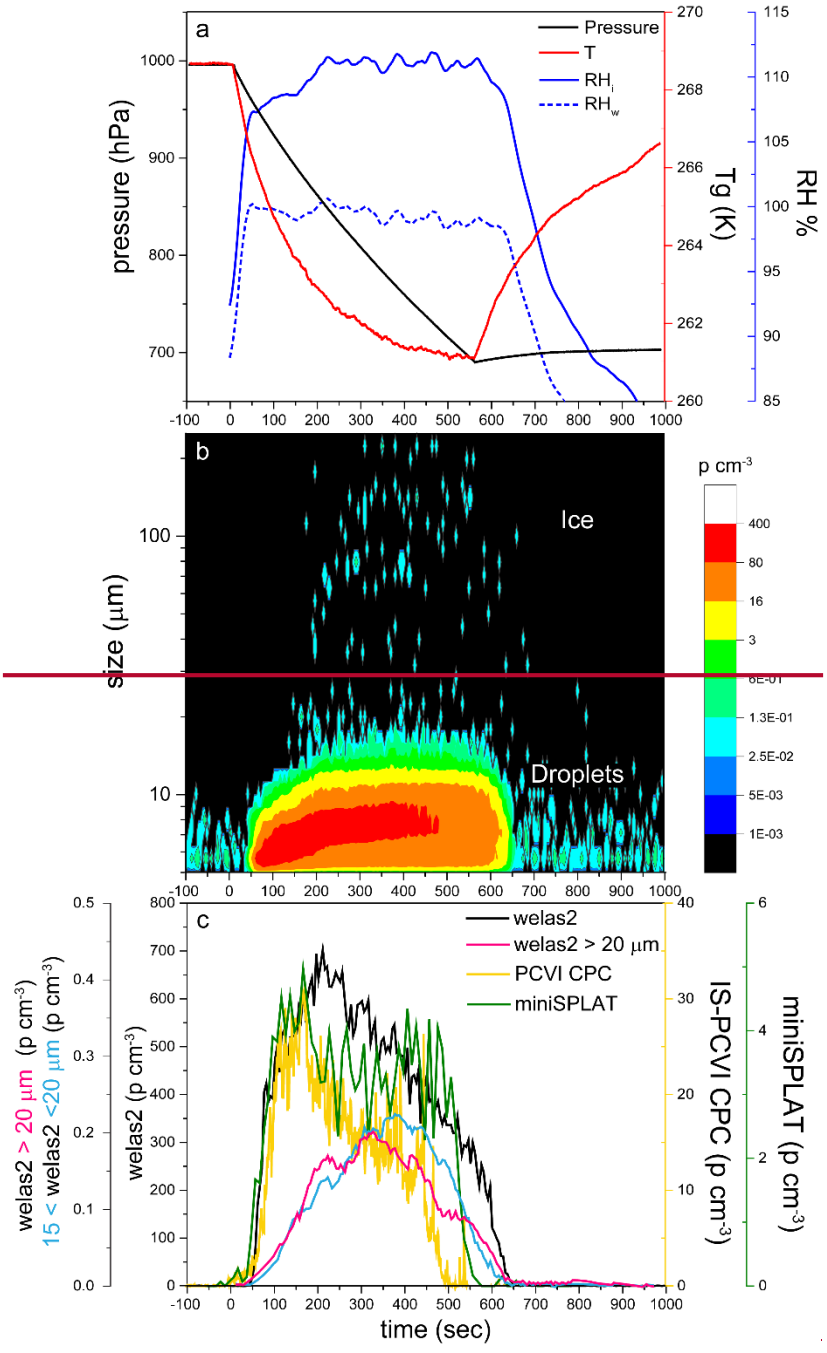
a
Pressure
T
RH$_i$
RH$_w$
pressure (hPa)
Tg (K)
RH %
b
Ice
Droplets
size (µm)
p cm^{-3}
400
80
16
3
1.3E-01
2.5E-02
5E-03
1E-03
c
welas2
welas2 > 20 µm
PCVI CPC
miniSPLAT
welas2 > 20 µm (p cm^{-3})
15 < welas2 <20 µm (p cm^{-3})
welas2 (p cm^{-3})
IS-PCVI CPC (p cm^{-3})
miniSPLAT (p cm^{-3})
time (sec)

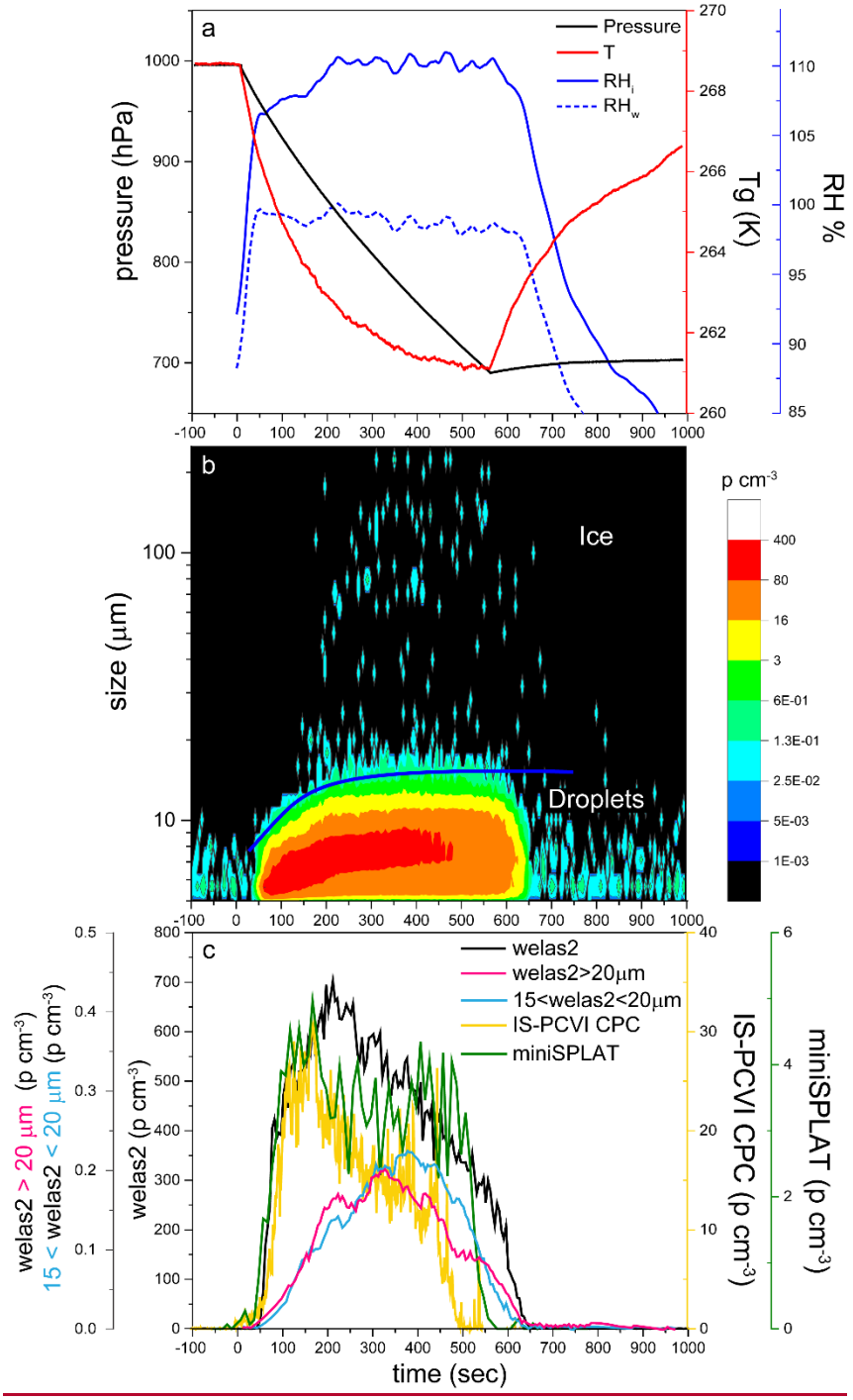

Figure 1~~3~~2: Data from Expansion 3 with PF CGina bacteria. (a) The pressure (black) and the temperature of the gas (red) inside the AIDA chamber. The measured RH with respect to ice (RHi) and water (RHw) are indicated in solid and dashed blue lines, respectively; (b) the size distributions of the particles measured with welas2 during the expansion. Particles smaller than ~15 µm are liquid droplets, while larger particles are ice. The IS-PCVI cut-size is shown in blue; (c) The welas2-measured total particle number

concentrations (black), the welas-2 number concentrations of particles larger than 15 µm, but smaller than 20 µm (light blue), and the welas-2 number concentrations of particles larger than 20 µm (pink). The CPC and miniSPLAT measured number concentrations of particles transmitted by the IS-PCVI are marked in yellow and green, respectively.

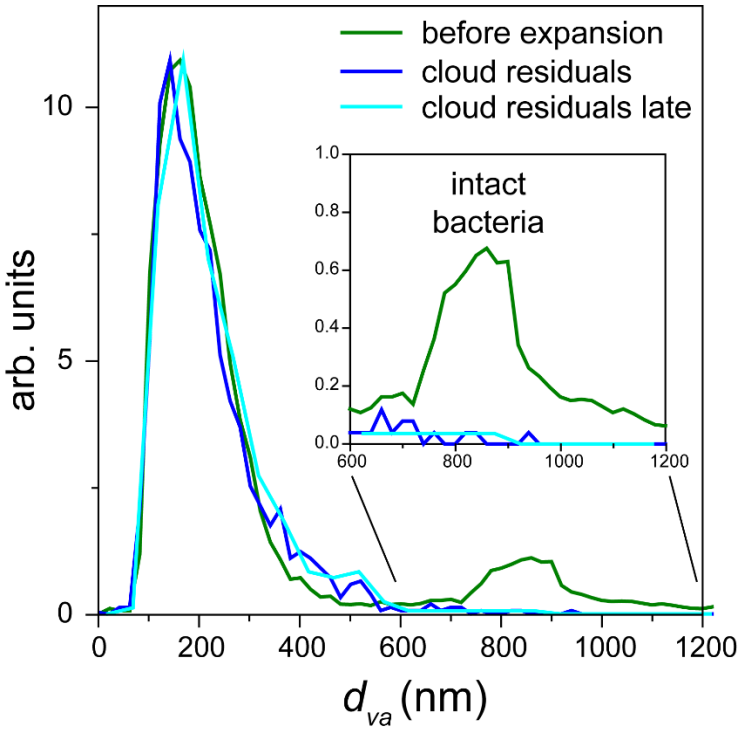

Figure 143: d_{va} size distribution measured by miniSPLAT before Expansion 3 (green) with PF CGina bacteria, of cloud residuals (blue), and of cloud residuals measured during the later part of the expansion (302-557 seconds) when the number concentration of sampled droplets and ice crystals were nearly the same (light blue). The inset shows an expanded scale of the region of intact bacteria.

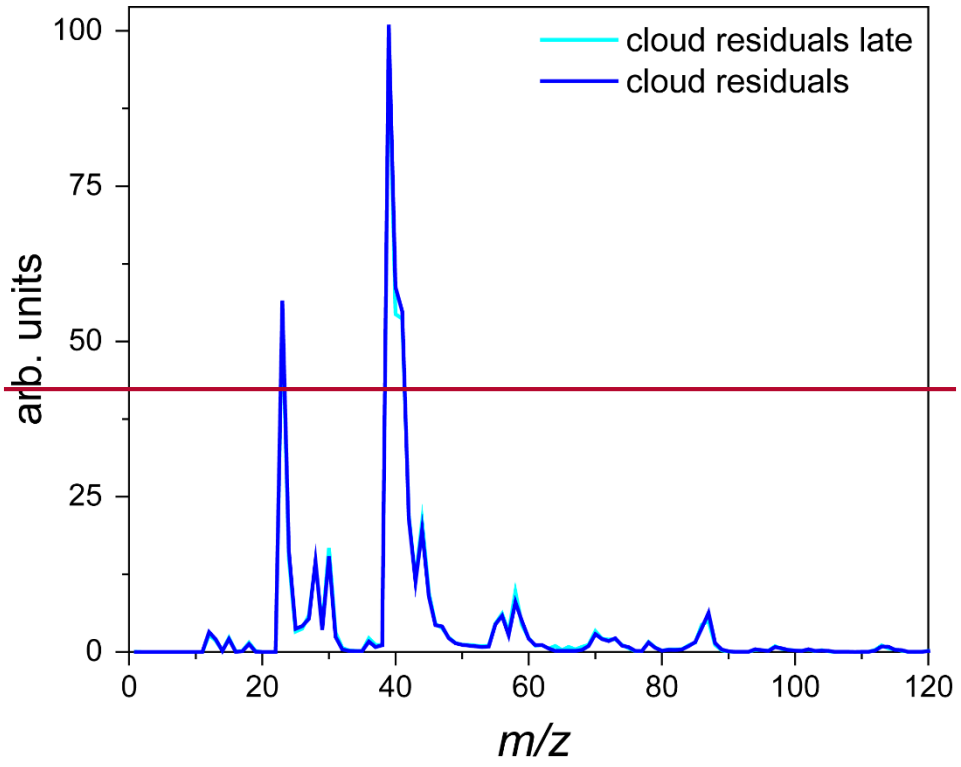
cloud residuals late
cloud residuals
arb. units
m/z
0
25
50
75
100
0
20
40
60
80
100
120

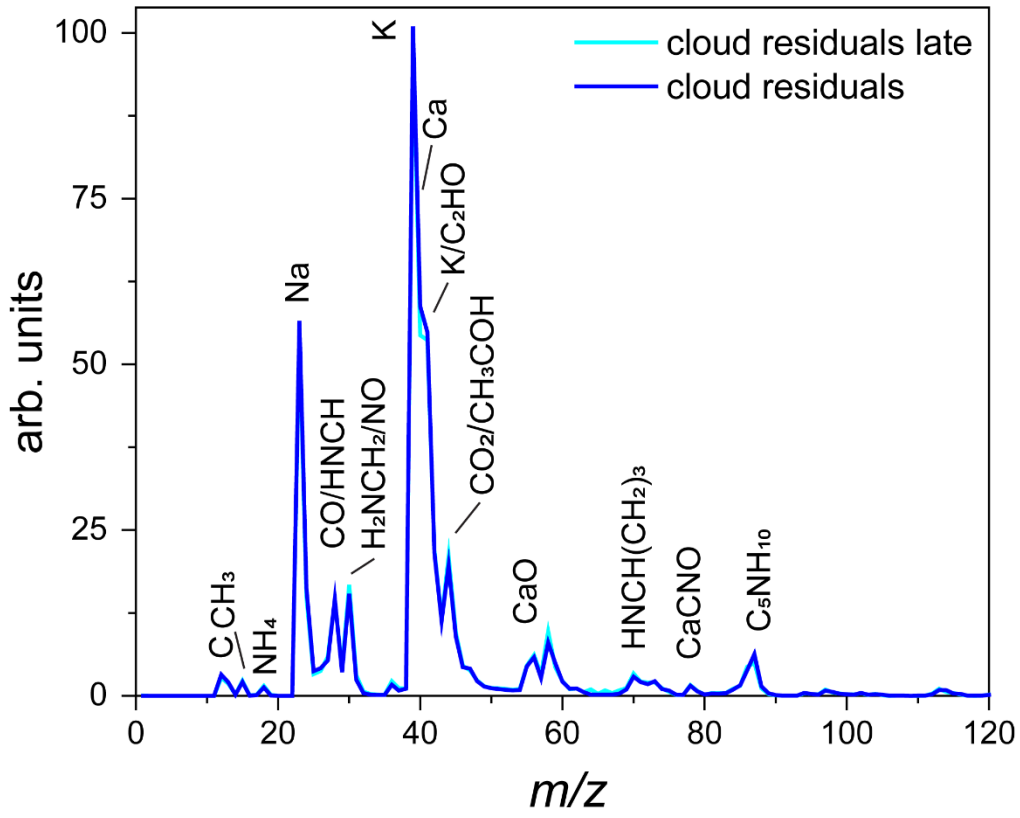

Figure 154: Average mass spectrum of cloud residuals measured during Expansion 3 (blue) with PF CGina bacteria super imposed on the average mass spectrum of particles characterized later in the expansion (302-557 seconds) when the number of sampled ice crystals and cloud droplets were comparable (light blue).